HEAT AND MASS TRANSFER ANALOGY UNDER TURBULENT CONDITIONS OF FRYING

A Thesis Submitted to the

College of Graduate Studies and Research

In Partial Fulfillment of the Requirements

For the Degree of Master of Science

In the Department of Agricultural and Bioresource Engineering

University of Saskatchewan

Saskatoon, Saskatchewan

By

Adefemi Farinu

PERMISSION TO USE

In presenting this thesis in partial fulfillment of the requirements for a Postgraduate degree from the University of Saskatchewan, I agree that the Libraries of this University may make it freely available for inspection. I further agree to permission for copying of this thesis in any manner, in whole or part, for scholarly purposes as may be granted by the professor who supervised my thesis work, or in his absence, by the Head of the Department or the Dean of the College in which my thesis work was done. It is understood that any copying or publication or use of this thesis or parts thereof for financial gain shall not be allowed without my written permission. It is also understood that due recognition shall be given to me and to the University of Saskatchewan in any scholarly use which may be made of any material in my thesis.

Requests for permission to copy or to make other use of material in this thesis in whole or in part should be addressed to:

Head, Department of Agricultural and Bioresource Engineering
University of Saskatchewan
Saskatoon, Saskatchewan
S7N 5A9
CANADA

ABSTRACT

Sweetpotato (*Ipomoea batatas*) is a popular vegetable across the world. It is a staple food item of many countries in South America, Africa and Asia where the population depends on the crop as an important source of energy and essential nutrients like vitamins A and C, calcium, iron and copper. It is also a very popular crop in North America. Deep fat frying is one of the favourite processing methods for sweetpotato. The method is fast and the finished product is desired for its unique flavour and taste.

The main objective of this study was to establish analogy between convective heat and mass transfer during frying. The accurate estimation of the coefficients for both phenomena is challenging. During frying, the rate of heat transfer from the oil to the food surface is largely controlled by the convective heat transfer coefficient. This heat transfer coefficient is dependent on the interaction between the temperature gradient and the drying rate in a frying process. The temperature gradient and the drying rate in turn partly depend on the thermophysical properties of the product. In this study, thermophysical properties of sweetpotato were studied and modeled as a function of moisture content and temperature. The properties of interest are specific heat capacity, thermal conductivity, thermal diffusivity and density. A designed deep fat frying experiment of sweetpotato was carried out under four different oil temperatures (150, 160, 170 and 180°C) and using three different sample sizes (defined as ratio of diameter to thickness, D/L: 2.5, 3.5 and 4.0). Convective heat transfer coefficients under these frying conditions were estimated and computer

simulation based on finite element modeling technique was used to determine convective mass transfer coefficients. Correlation between heat transfer coefficient and mass transfer coefficient were investigated with reliable statistical tool. Effects of sample size, oil temperature and frying time on heat and mass transfer were also studied.

Specific heat, thermal conductivity and thermal diffusivity of sweetpotato were all found to increase with increase in temperature and moisture content. Density decreased with increase in moisture content. Maximum heat transfer coefficient reached during sweetpotato frying was in the range of 700-850 $W/m^{2}{}^{\circ}C$. Heat transfer coefficient of sample during frying increased with increase in frying oil temperature but decreased with increase in sample size. Same trend for heat transfer coefficient was observed for effects of oil temperature and sample size on mass transfer coefficient. Maximum mass transfer coefficient reached during sweetpotato frying was in the range of 4×10^{-6} to 7.2×10^{-6} $kg/m^{2}.s$. No general relationship was established between heat transfer coefficient and mass transfer coefficient during frying but a relationship was established between maximum heat transfer coefficient and maximum mass transfer coefficient. A trend was also observed between maximum heat transfer coefficient and the corresponding mass transfer coefficient at that point.

ACKNOWLEDGEMENT

I am indebted to my supervisor Dr. Oon-Doo Baik. I owe to him the opportunity for this study in the first place. His extreme patience, constant encouragement and infectious enthusiasm made all the difference in completing this study.

I would like to express my gratitude to my graduate committee members Dr. Venkatesh Meda and Dr. Lope Tabil Jr. for sharing their wealth of knowledge with me and making themselves available for guidance at various stages of this program.

I would also like to thank Natural Sciences and Engineering Research Council of Canada (NSERC) for financial support and Agriculture and Agri-Food Canada for providing equipment for Specific heat measurement. I would like to thank the department of Agricultural and Bioresource Engineering, University of Saskatchewan as a whole and my colleagues for the opportunity, academic and moral support. I must mention Wayne Morley, Louis Roth, Toni Schleicher and Bill Crerar for their technical helps in my experiments, and Pat Hunchak for christening me after a Legend (Michael Jordan) on my first day in the department.

My appreciation goes to friends in Canada: Yinka, Samuel, Jide, Taiwo, Lekan, Tope, Paul, Ebenezer, Dapo and friends in Nigeria: Noble brothers. Specific mention of Gbola Oladokun is necessary.

My utmost thanks go to Jehovah. He is indeed faithful.

DEDICATION

This thesis work is dedicated to my family: Ajibade, Bolanle, Adeyinka, Adedoyin, Adedunmola, Oluwaseun and also to Juliet.

TABLE OF CONTENTS

LIST OF FIGURES

LIST OF TABLES

NOMENCLATURE

A = area (m^2)

c = concentration (kg/m^3)

C_m = specific moisture capacity ($kg_{moisture}/kg_{sample}$)

C_p = specific heat (J/kg.K)

d = sample diameter to thickness ratio *i.e.* D/L

D = mass diffusivity (m^2/s)

h = heat transfer coefficient ($W/m^2.K$)

h_m = mass transfer coefficient ($kg/m^2.s$)

$\dot{I}$ = volumetric expansion ($kg/m^3.s$)

k = thermal conductivity (W/m.K)

k_i = the thermal conductivity of *ith* phase

k_m = moisture conductivity (kg/m.s)

L = length of material (m)

m = moisture content (wet basis)

m_w = moisture content (g water/g solid).

M = mass of material (kg)

M_f = oil content (% wet basis)

mfep = equilibrium fat content (mass fraction, dry basis)

n = mass flux (kg/m^2)

KL = fat conductivity (m/s)

P = Pressure (Pa)

Pr = Prandtl number

q = heat flux (W/m^2)

Q = heat lost or gained (J)

R = radius (m)

r = radial distance (m)

Sc = Schmidt number

S = saturation

T = temperature (°C)

t = time (s)

T_o = oil temperature (°C)

T_s = surface temperature (°C)

U = velocity (m/s^2)

V = product volume (m^3)

v = kinematic viscosity (m^2/s)

V_p = volume of the sample (cm^3)

V_c = volume of the cell containing the sample (cm^3)

V_R = volume of the reference cell (cm^3)

x = material thickness (m)

X_i^w = mass fraction of food component i.

X_i^v = volume fraction of component i

α = thermal diffusivity (m^2/s)

μ = dynamic viscosity (kg/m.s)

Ψ = dimensionless distance

ρ = density (kg/m^3)

ϕ = porosity

θ_{abs} = absolute temperature (K)

λ = latent heat of evaporation of water (J/kg)

ε_i = Volume fraction of specie i (m_i^3 / m_t^3)

Subscripts: *v, w, a, o, g, s, p, and eff* are vapour, water, air, oil, gas (vapour+air), solid matrix (surface), partial pressure, and effective, respectively.

1. INTRODUCTION

1.1 Background

Sweetpotato (*Ipomoea batatas*) is a crop whose large starchy sweet tasting tuberous root is an important vegetable. It is not particularly related to the regular potato, which is sometimes called the Irish potato to distinguish it. The two crops are from different families. In rating 58 vegetables by adding up the percentages of recommended daily allowance (RDA) for six nutrients (Vitamin A and C, folate, iron, copper and calcium), plus fibre, the Nutrition Action Health Letter rated sweetpotato the highest with 582 points; its nearest competitor, a raw carrot came in at 434. Also, the Centre for Science in the Public Interest rated the relative nutritional value of common vegetables and once again, the sweetpotato came out on top with a score of 184, as compared with a similarly prepared regular potato, which scored only 83 points (Rodriguez *et. al.,* 1975). Sweetpotato's processing has not been fully studied yet despite its popularity and importance all over the world.

Deep fat frying is a very important and popular method of food processing. The snack industry in North America and all other part of the world is a multi-billion dollar venture and deep fat fried foods are at the center of this industry. Despite health concerns for fried foods in terms of high cholesterol content of

some oil used in deep frying, they are still craved for the unique flavour and speed of the process.

Deep fat fried sweetpotato is popular all over the world. In this process, sweetpotato slices are cooked by immersion in an edible fat or oil at temperature between 150 and 200°C. During the frying process, heat and mass transfer within the product occurs simultaneously. Heat and oil are transferred from the frying medium to the sweet potato while moisture is transferred from the product to the frying oil. The quality of the fried product depends on the frying process.

Frying is a very turbulent process ($Re > 5 \times 10^5$). Turbulence is associated with the existence of random fluctuations in the fluid. Transport of heat, mass and momentum in a turbulent boundary layer is attributed to motion of eddies, which are small portion of fluid in the boundary layer that move about for a short time before losing their identity. Because of this motion, the transport of energy mass and momentum is greatly enhanced. The existence of turbulence therefore is advantageous in providing increased heat and mass transfer rates. However, it makes the process more complicated to describe theoretically. In modeling the frying process, there is a need to determine the convective boundary conditions in heat and mass transfer. The factors that govern the rate of heat and mass transfer during frying are the heat transfer coefficient and mass transfer coefficient and they are interrelated for a particular process. The oil temperature during frying as well as the thermal and physical characteristics of the product and those of the oil is important in determining these coefficients. Most deep fat frying studies in literature focussed on determining heat transfer coefficient. Studies that actually quantified the

corresponding mass transfer coefficient and investigated the link between the two coefficients are very scarce.

1.2 Statement of the problem

The relationship between heat transfer coefficient and mass transfer coefficient is very important in determining the rate of heat and mass transfer during deep fat frying. Since mass transfer in a food product is driven by the heat transferred to the product, both are interwoven and establishing the relationship between them is vital to understanding the dynamics of the process and predicting the rate. Studies on heat and mass transfer analogy under both laminar and turbulent conditions exist in literature. However, no model has been developed yet for the special case of frying. The turbulent nature of the process by the bubbling action and the structural changes that accompanies a fried product make the process both fascinating and challenging. Available information in literature on processing of sweetpotato does not justify the importance of the crop. This thesis work hopes to fill this gap.

1.3 Objectives

The general objective of this study is to develop heat and mass transfer analogy during deep fat frying of sweetpotato based on a finite element method computer simulation.

The specific objectives are:

1. to model the thermophysical properties of sweetpotato as a function of product temperature and moisture content;

2. to determine the convective heat transfer coefficient of deep fat fried sweetpotato from temperature and moisture content profiles of a designed experiment;
3. to simulate sweetpotato frying and determine convective mass transfer coefficient using a finite element method based numerical model; and
4. to develop an empirical correlation between heat transfer coefficient and mass transfer coefficient during frying based on geometries and oil temperatures applied and investigate the effects of these factors on the coefficients.

2. LITERATURE REVIEW

This chapter reviews research work along the areas of this study found in literature. It is basically a review on sweetpotato, thermophysical properties measurement, deep fat frying process, mathematical modeling and simulation of deep fat frying process and heat and mass transfer analogy.

2.1 Sweetpotato

Sweetpotato (*Ipomoea batatas*) belongs to the *Convolvulaceae* or morning-glory family and is a dicot (having a two-leafed embryo). The genus consists of more than 400 species of which, more than 200 occur in tropical America (Charney and Seelig, 1967). It is a tuberous-rooted perennial crop. Its stems are usually prostrate and slender. The root does not have eyes or scars as found on some other roots and tubers, but it possesses the ability to develop adventitious buds on sprouts or vine cuttings, which is advantageous in reproducing the crop by vegetative means (Charney and Seelig, 1967). History has it that Columbus and his shipmates found the native-American plant and mentioned it on their fourth voyage (1502-1504). The Incas of South America and Mayas of Central America grew several varieties and called the plant *cassiri*. Sweetpotato reached St. Thomas off the African coast before 1574. It is

believed that early Spanish explorers took the sweetpotato to the Philippines and the East Indies, after which Portuguese voyagers carried it to India, China and Malaya (Charney and Seelig, 1967).

Both yellow and white types of sweetpotato exist, the colour being of the flesh. The yellow type is preferred because of the attractive colour, good flavour and cooking qualities (Rodriguez et. al. 1975). However it is not as sweet as the white type. Sweetpotato is an exceptionally rich source of Vitamin A (7100 IU/100 g). It also has appreciable quantities of ascorbic acid, thiamine, riboflavin, niacin, phosphorus, iron and calcium (U.S.D.A, 1984; Picha, 1985). Sweetpotatoes are usually consumed after baking, boiling, steaming, frying or it may be candied with syrup, sliced into chips, or pureed. Deep fat frying is one of the popular methods of processing sweetpotato. It is used to produce French fries or chips.

2.2 Thermophysical properties

The knowledge of thermal and physical properties is essential for thermodynamic research and modeling the heat treatment of foods including vegetables. This is because the properties, to a large extent, determine the rate of the heat transfer process. Previously, constant average values of thermal properties were used in analyses of food processes, which have lead to inaccuracies since these properties actually change during the process. However, modern analytical techniques have made it possible to accommodate these dynamic changes. The most important thermo-physical properties in food

processing, specific heat capacity, thermal conductivity, density and thermal diffusivity of food materials depend mostly on the food's composition, temperature and density (Choi and Okos, 1985). A lot of work has been done on thermal properties of vegetables; Irish-potato for instance, but very little work has been done on thermal properties of sweetpotato. Related research works found in literature are discussed in this section

2.2.1 Specific heat capacity

The specific heat of a substance represents the variation of temperature with the amount of heat stored within the substance. It depends on the nature of the heat addition process in terms of either a constant pressure or a constant volume process. However since pressure change in heat transfer problems of food materials are usually very small, the specific heat at constant pressure is most often considered. Specific heat is the ratio of heat loss or gained to temperature change for a unit mass. Mathematically, it can be represented as;

$$C_p = \frac{Q}{M\Delta T} \qquad (2.1)$$

Where

Q = heat lost or gained (J),

M = mass of product (kg),

ΔT = temperature change in the food material (K),

C_p = specific heat (J/kg.K).

The need for reliable specific heat data for food materials has been recognised for a long time. Siebel (1892) proposed that the specific heat of food materials such as fruits, eggs, vegetables and meat could be assumed equal to the specific heat of water and that of the solid matter in combination with water. Siebel (1892) proposed the following equation for food at temperature above freezing point:

$$C_p = 0.008m + 0.2 \qquad (2.2)$$

Where:

C_p = specific heat capacity of the food (Btu/lb.°F)

m = moisture content of the material (percentage wet basis);

0.2 = a constant assumed to be specific heat of dry solid in the food.

Stitt and Kennedy (1945) suggested that the constant in the Siebel equation (equation 2.2) be changed from 0.2 to 0.32 for temperature range of 32°F to 77°F and 0.45 for temperature range of 77°F to 149°F. Sweat (1986), however, noted that both Siebel's linear model and the modification made by Stitt and Kennedy (1945) gave significant deviation from experimental results at lower temperature. Hence the application of the models was divided into two ranges, one above M.C of 50% (w.b.) and one below 50% (w.b.).

Choi and Okos (1983) developed a specific heat model which takes into account the individual contribution of major food components:

$$C_p = 4180X_w^w + 1711\,X_p^w + 1928\,X_f^w + 1547\,X_c^w + 908\,X_a^w \qquad (2.3)$$

Where:

C_p = specific heat of food (J/kg.K)

X^w= mass fraction of each component.

Subscripts *w, p, f, c* and *a* are water, protein, fat, carbohydrate and ash, respectively.

Methods of mixtures and differential scanning calorimetry are the most common experimental methods used for specific heat determination of food materials. Hwang and Hayakawa (1979) used a calorimeter to measure the specific heat of food materials. The authors avoided direct contact between food and the exchange medium in the calorimeter. Two rubber O-rings were introduced into the calorimeter to prevent water loss by evaporation. Gupta (1990) reported a simpler calorimeter than that of Hwang and Hayakawa (1979). In this study, the test capsule was made of copper tube with rubber stoppers at both end of the tube. Gupta (1990) mentioned that the specific heat above 100°C can be measured by using vegetable oil or mineral oil as the heating medium in place of water.

The method of differential scanning calorimetry, DSC is more advanced and has enjoyed a wide application in determining the specific heat of food materials. Moreira *et. al.* (1995) used DSC to determine the specific heat of tortilla chips as a function of frying time. Scanning was conducted at a heating rate of 12°C/min. C_p of tortilla chip from this study ranged from 2560 to 3360 J/kg.K. Kramkowski and co-worker (2001) determined the specific heat of garlic as a function of temperature at different moisture content levels. Specific heat was found to increase with temperature ranging from 2400 to 4100 J/kg.K. Tang

and co-workers (1991) used DSC to determine the specific heat capacity of lentil seeds. Specific heat values of lentil seed increased quadratically with moisture content over the range of 2.1 to 25.8% w.b. and a linear increase with temperature varying between 10 and 80°C. Wang and Brennan (1993) determined specific heat of potato using DSC and model C_p as a function of moisture content and temperature. C_p of potato was reported to increase quadratically with moisture content over the range 0-4.13 (g water/g solid) and increased linearly with temperature varying from 40 to 70°C. Model proposed for C_p of potato is given in equation (2.4)

$$C_p = 0.406 + 0.00146T + 0.203m_w - 0.0249m_w^2 \quad (2.4)$$

Where:

C_p = Specific heat (cal/g.°C)

T = Temperature (°C)

m_w = moisture content (g water/g solid).

2.2.2 Thermal conductivity

Thermal conductivity, k of a material gives the amount of heat that will be conducted per unit time through a unit thickness of that material, if a unit temperature gradient exists across that thickness. Thermal conductivity can be either determined experimentally or through mathematical estimation. Woodside and Messmer (1961) and Brailsford and Major (1958) both determined the maximum and minimum thermal conductivity of a two-phase system as series (two phases are thermally in series with respect to the direction of heat flow) and

parallel (two phases are thermally in parallel with respect to the direction of heat flow) distribution.

Series model is represented by:

$$\frac{1}{k} = \sum_{i=1}^{n} \frac{X_i^v}{k_i} \qquad (2.5)$$

While the parallel model is represented by:

$$k = \sum_{i=1}^{n} X_i^v k_i \qquad (2.6)$$

Where:

X_i^v = the volume fraction of *ith* component phase (m^3)

k_i = the thermal conductivity of *ith* phase (W/m.K)

k = thermal conductivity of the product (composite medium) (W/m.K).

Murakami and Okos (1989) considered thermal properties of 15 different food powders from literature and observed that all data points fall on the range defined by values predicted by series and parallel models. It was observed that the parallel model defined the upper limit while the series model defined the lower limit of the predictions.

Generally, there are two broad methods of experimental measurement of thermal conductivity in literature. The steady-state methods are based on the Fourier's law of steady state heat conduction. The method is mathematically simple and is quite accurate for dry, granular and solid food. The major disadvantages of steady-state methods are the long time required to attain steady-state conditions and the possibility of moisture migration due to temperature gradient across the material. Transient methods of thermal

conductivity measurement make use of the governing equations for the temperature history in a solid body. Transient methods require a short time for measurement, which also reduces the chances of moisture migration.

Both steady-state and the transient methods have been used extensively in food applications. Saravacos and Pilsworth (1965) used the guarded hot plate for thermal conductivity measurement of several freeze-dried gels and determined *k* from the following equation:

$$k = \frac{qx}{A\Delta T} \qquad (2.7)$$

Where:

k = thermal conductivity (W/m.K)

q = rate of heat input (W)

x = material thickness parallel to heat flow (m)

ΔT = temperature change (°C)

A = contact area normal to direction of heat flow (m^2).

Farral and co-workers (1970) determined the thermal conductivity of various types of spray-dried and drum-dried powdered milks using the concentric cylinder method and the following equation:

$$k = \frac{q \ln\left(\frac{r_2}{r_1}\right)}{2\pi L\left(T_1 - T_2\right)} \qquad (2.8)$$

Where:

L = length of the cylinder (m),

T_1 and T_2 = the temperature of the material (K) at radii r_1 and r_2 (m) respectively,

q and *k* are as defined for equation (2.7).

Kazarian and Hall (1965) used the line source method to measure the thermal conductivity of yellow dent corn and soft white wheat. *k* was estimated using equation (2.9):

$$k = \frac{q}{4\pi L(T_1 - T_2)}.\ln\frac{t_2}{t_1} \qquad (2.9)$$

Where:

T_1 and T_2 = the temperature (K) at the time $t_1$and t_2 (s) after heating respectively,

q = rate of heat input (W),

k = thermal conductivity (W/m.K),

L = length of material (m).

Wang and Brennan (1992) measured thermal conductivity, *k* of potato using line-source probe. Thermal conductivity was determined at various moisture contents (0-4.7 g water/g solid) and in temperature range of 40-70°C. *k* of potato was reported to decrease with moisture content and was correlated with moisture content by a semi-logarithmic equation. The authors reported that temperature had little effect on *k* in the temperature range used. Califano and Calvelo (1991) estimated thermal conductivity of potato from heat penetration into cylindrical samples between 50 and 100°C. *k* was found to range from 0.545 to 0.957 W/m°C for potato with specific gravity of 1070 kg/m^3 and moisture content of 80%. *k* also varied with temperature quadratically.

2.2.3 Thermal Diffusivity

The rate at which heat diffuses through a material is determined by

thermal diffusivity, α of the material. The property gives a measure of how quickly a material's temperature will change when the material is heated or cooled. It gives the ratio of conducted energy to stored energy in a material. Thermal diffusivity can either be determined from direct measurement or estimated from thermal conductivity, density and specific heat data. For direct methods, thermal diffusivity is usually determined from the solution of one-dimensional unsteady state heat transport equation with the appropriate boundary conditions for infinite and finite bodies by analytical methods and for irregular bodies by numerical methods. Indirect estimation of thermal diffusivity needs considerable time and different instruments since a variety of properties have to be determined independently. Kazarian and Hall (1965) directly measured thermal diffusivity of yellow dent corn and soft white wheat. Arce and co-workers (1981) determined the thermal diffusivity of defatted soy flour indirectly from thermal conductivity, specific heat and mass density data:

$$\alpha = \frac{k}{\rho C_p} \qquad (2.10)$$

Where:

k = thermal conductivity (W/m.K),

ρ = mass density (kg/m^3),

C_p = specific heat capacity (J/kg.K),

α = thermal diffusivity (m^2/s).

Drouzas and co-workers (1991) used direct (probe method) and indirect method to determine the thermal diffusivity of granular starch and found that indirect method yielded more accurate values than the direct measurement as

concluded from F-test at 5% significance level. Wadsworth and Spadaro (1969) reported a thermal diffusivity value of 1.1×10^{-7} m^2/s for sweetpotato. The authors heated sweetpotato in a constant temperature water bath at 55, 70, 80 and 90°C and calculated thermal diffusivity from the experimental time-temperature curve. It was further reported that t thermal diffusivity of sweetpotato increased with temperature while cooking due to increase in thermal conductivity and changes in starch structure, mainly, starch gelatinization. Thermal diffusivity, however, started decreasing with temperature increase after 90°C as starch cells in sweetpotato became distended, weakened and cell walls started to separate with starch molecules being hydrolyzed.

2.2.4 Density

Density is the ratio of mass to volume of a material. Density of food products is an important property in analyzing food processing unit operations. It is closely related to porosity and moisture content of food. True density is the density of a pure substance or a material calculated from its components' densities considering conservation of mass and volume. Most density measurement applications usually borders around volume measurement since density is the ratio of mass to volume. Measuring the true volume of food products is challenging due to the irregularity in shapes or characteristic dimension of most biomaterials and voids in the product that had to be accounted for. A method that has been used for measuring apparent density of irregular-shaped product is buoyant force determination (Rahman, 1995). In this

procedure, a sample is suspended in a liquid of known density and the weight of the sample inside the liquid is measured. Buoyant force is the difference between the mass in air and the mass in liquid. Apparent density ρ_{ap} is then determined from equation (2.11):

$$\rho_{ap} = \rho_l \frac{W}{G} \qquad (2.11)$$

Where:

W and G = weight of sample in air and buoyant force respectively (N)

ρ_l = density of liquid (kg/m^3)

ρ_{ap} = apparent density of sample (kg/m^3).

For most food products, there is exchange of solid, liquid or gas from the sample when suspended in a liquid and this could be prevented by enclosing the sample in cellophane or by coating a thin layer of varnish or wax on the sample (Rahman, 1995). Volume of a sample can also be determined by measurement of liquid volume displaced using a specific gravity bottle. Mohsenin (1970) mentioned the characteristics of a liquid preferred when using this method as little tendency to soak sample, smooth flow, low solvent action, high boiling point, stable and low specific gravity when exposed to atmosphere. An example of such liquid is toluene. Gas pycnometer is a good method of measuring porous and non-porous solids. The device measures volume by using high pressure gas. Sabapathy (2005) determined particle density of Kabuli chickpea with a gas multipycnometer at seven levels of moisture content. The author reported that density decreased with increased moisture content.

2.2.5 Moisture Diffusivity

Moisture diffusivity is a measure of a product's tendency to produce entropy when it is disturbed from equilibrium by imposition of a concentration gradient. It is defined as the proportionality constant between a flux and a driving flux (Kestin and Wakeham, 1988). For any drying application an example of which is frying, the internal moisture migrates towards the external surface of the product by means of a number of mechanisms such as diffusion, capillarity and sequences of evaporation-condensation. Generally, two or more of these mechanisms occur simultaneously, making rigorous theoretical modeling of drying kinetics quite difficult due to variable transfer phenomena coefficients. Fick's second law of diffusion (equation 2.12) is widely used to gather all of the mass transfer mechanisms into one equivalent moisture transport coefficient (Derdour and Desmorieux, 2004).

$$\frac{\partial c}{\partial t} = \frac{\partial}{\partial x}\left(D \frac{\partial c}{\partial x} \right) \qquad (2.12)$$

Where:

c = concentration (kg/m^3)

t = time (s)

x = material thickness along direction of mass transfer (m)

D = diffusion coefficient (m^2/s)

There is no standard method for moisture diffusivity estimation, although most of the available methods are based on Fick's laws of diffusion. The differences among the methods include the kind and the conditions of experiments used (simple or sophisticated setups, permeation, sorption or

drying operation, various specimen geometries) and the treatment of experimental data. Most of the moisture diffusivity data available originate from the method of drying curves. What is usually meant by a drying curve is the representation of change in moisture content of a food specimen with time or the change in the drying rate with moisture content. Depending on the material and drying conditions, the drying curve may adopt different shapes. The relationship between diffusivity and the product temperature is often of the Arrhenius type. *D* values for potato exist in literature. For temperature range of 418K to 458K, moisture diffusivity of potato is given by equation (2.13) (Rice and Gamble, 1989):

$$D = 11.04 \exp\left(-\frac{2911}{\theta_{abs}} \right) \qquad (2.13)$$

Where:

D = moisture diffusivity (m^2/s)

θ_{abs} = absolute temperature (K)

2.3 Deep Fat Frying

Deep fat or immersion frying is defined as the process of cooking foods by immersing them in edible fat or oil, which is at a temperature above the boiling point of water, usually 150-200°C (Farkas *et al.*, 1996a). The process involves simultaneous heat and mass transfer which makes it a complex process to study and analyse.

2.3.1 The frying process

Deep fat frying as a method of food processing combines high processing speed with good product appearance, although lower yield and higher fat content was also reported for the method. Deep fat frying is a very fast method of food processing among conventional heat transfer methods. Bengtsson and Jacobsson (1974) reported deep fat frying at oil temperatures normally used for the process as the fastest of three methods: deep fat frying, IR heating and pan-frying at normal operating conditions when meat patties of 10 mm thickness was fried.

Deep fat frying is considered a moving boundary problem, where a previously non-existent crust region develops on the food surface and increases in thickness inwards during frying while the core region decreases with frying time. The process was broken down into four stages by Farkas and co-workers (1996a). The first stage, known as initial heating, is the period of time within which the surface of the product is heated from its initial temperature to the boiling point of water. This phase is usually short and a negligible amount of water is lost from the food. The second stage, surface boiling, is noted for rapid loss of surface free moisture, an increase in surface heat transfer coefficient and beginning of crust formation. The falling rate stage represents the period of time during which the bulk of the moisture is lost. It is the longest of the stages and the temperature of the core region approaches that of boiling point of water. Bubble end point is the final stage of frying. It describes the apparent end of moisture loss from the product during frying.

The following factors were found to govern the process rate in deep fat frying and also affect the quality of the fried product: the thermophysical properties of the food and those of the oil, the temperature of the oil, the geometry of the food and finally, the processing conditions that are likely to lead to the degradation of the oil in the process (Moreira *et. al*., 1995a).

2.3.2 Heat Transfer

During deep fat frying of food, heat is transferred from the oil to the surface of the food immersed in it by convection and onward from the food surface to its geometric centre by a combination of conduction and advection. Liquid water moves from inside the food outwards and on reaching an established evaporation front, turns to vapour and leaves surface as vapour. Once the moisture on the surface of a food has been removed in a deep fat frying process, a crust begins to form and its thickness increases over the duration of frying. The crust reduces the rate at which water is vaporized and food is cooked (Farkas *et al.*, 1996a). The rate of temperature change within the core region is only slightly affected by the external oil temperature due to an isotherm at a slightly elevated water boiling point at the crust/core interface (Farkas *et. al.,* 1994). Hubbard and Farkas (1999) divided frying process into two phases with bubbling action: non-boiling phase (made up of the initial heating and the bubble end point stages) and the boiling phase (made up of the surface boiling and the falling rate stages)

The rate of heat transfer from the oil to the food is controlled by the surface heat transfer coefficient, *h* at the boundary between the food and the oil. Convective heat transfer coefficients for the non-boiling phase have been found to be in the range of 250-300 W/m^2°C (Moreira *et. al.*, 1995a; Miller *et. al.,* 1994). Values of 300 W/m^2°C at the onset of boiling and a peak value of 1100±140 W/m^2°C during frying have also been reported (Hubbard and Farkas, 1999).

Baik and Mittal (2002) determined and analyzed *h* at two locations (top and bottom surfaces) of a tofu disc during frying based on energy and mass balance. It was reported, in this study, that the top surface temperatures were lower than those of the bottom in the beginning of frying (less than 40-600 s) at 147-172°C oil temperature. Later, temperatures at the top surface exceeded those at the bottom. The authors reported that *h* for the bottom surface was higher at the beginning and it was attributed to different magnitudes of natural convection at the two portions without significant bubble release at the onset of frying. After vapour release, *h* at the top surface was higher than that for the bottom surface for all frying cases. The authors speculated that the higher magnitude of agitation at the top surface resulted in the higher *h* value.

Moreira and co-workers (1995a) reported that convective heat transfer coefficient is dependent on the interaction between the temperature gradient and the drying rate in a frying process. As the thermal gradient between the oil and food increases, vapour loss rate also increased which additionally serve to further agitate the surrounding oil and increase the heat transfer coefficient. Increase in oil temperature also leads to low oil viscosity and hence its

resistance to flow, thereby further enhancing the heat transfer coefficient. It was reported that *h* value during frying is affected by bubble flow direction, velocity, bubble frequency and magnitude of oil agitation (Baik and Mittal, 2002). A hypothesis linking the increase in heat flux with increasing oil degradation through a reduction in the vapour bubble size and increase in the bubble frequency has been suggested (Farkas and Hubbard, 2000).

Tong and Tang (1997) found that formation and departure of vapour bubbles during boiling enhances heat flux to a material by forced convection of fluid across the material. However, the presence of bubbles on the food surface during frying insulates the surface from the heating media and can therefore reduce heat flux (Farkas and Hubbard, 2000). The effect of bubbling on the *h* value increases with the oil temperature during frying of potato. During the boiling phase, *h* values are 80% greater than those obtained without boiling for oil temperature of 180°C, while the increase in *h* value of boiling phase over non-boiling phase for oil temperature of 140°C is only 40% (Costa *et. al.,* 1999). This last observation can be attributed to the fact that higher temperature reduces the viscosity of the frying oil, which leads to further agitation of the frying process and thus, an increase in the *h* value. In this same study, the researchers also concluded that when moisture loss rate is high, the bubbles near the food surface may hinder the heat transfer since they serve as insulation pockets and also that the fraction of heat used for evaporation in a frying process depends on the temperature gradient between food and oil, water loss rate and the *h* value.

2.3.3 Moisture Transfer

Moisture loss during frying was expressed by the following general form (Rice and Gamble, 1989):

Rate of moisture transfer = Driving force**/**Resistance (2.14)

The driving force is provided by the conversion of water to steam, which forces its way out of the product while resistance to mass transfer is provided by internal resistance to mass diffusion and the surface resistance of the product. During frying, the free water at the surface of potato chips evaporated rapidly, the surface becomes dry and the inner moisture is converted to vapour, thereby, creating a vapour gradient (Rice and Gamble, 1989; Gamble and Rice, 1987, 1988).

Krokida and co-workers (2000) demonstrated that oil temperature has a negative effect on the moisture content of french-fried potatoes. As frying temperature increases, the moisture content for the same frying time decreases since an increase in temperature results in a higher kinetic energy for water molecules leading to a more rapid moisture loss in the form of vapour which ultimately reduces the moisture content of the product. Moisture removal rates were found to be higher in the top portion and at higher temperatures than in the bottom portion and at lower temperatures, respectively, during frying of a tofu disc (Baik and Mittal, 2002). Costa and co-workers (1999) used image analysis of bubbles to estimate water loss rate of potato during frying and observed a relationship between vapour build-up and water loss rate. Different flow patterns

were noticed for bubbles from top, side and bottom surfaces of potato during frying. Since this will lead to different agitation patterns, it was suggested that heat transfer coefficient might be expected to be position dependent. Also, there was a change in potato sample geometry during frying which also changed the oil agitation patterns and consequently changed the heat transfer coefficient. As frying proceeded, bubbling was found to increase to a maximum value and then decreased.

In a study on the effects of initial moisture content on sample temperature, moisture loss and crust thickness, Ni and Datta (1999) found moisture loss to increase significantly with initial moisture content because the surface evaporation and subsequent internal evaporation are much higher for high moisture food. The researchers also studied the vapour and liquid water fluxes in the crust and the core regions. For the crust region, it was reported that vapour diffused from the evaporation front to the product surface, with the maximum diffusional flux occurring near the evaporation front and its magnitude decreasing with the frying time since vapour concentration decreases with moisture content. In the core region, the capillary diffusional flux of water is towards the surface. There exist regions of constant flux where water saturation is spatially linear and capillary diffusivity is relatively constant. For the same core region, the authors also reported existence of water convective flux towards the center due to pressure. It has a smaller but comparable magnitude with capillary diffusional flux. It was concluded that neither transport mechanism in the core region could be ignored. Within oil temperature range of 145°C to 185°C, the

diffusion coefficients for moisture loss during frying of potato was found to increase from 58×10^{-10} to 109×10^{-10} m^2/s (Rice and Gamble 1989).

2.4 Mathematical modeling

Several mathematical models for frying at different levels of complexity have been reported. Rice and Gamble (1989) used analytical solution of Fick's second law to develop a one-dimensional diffusion model for potato slice frying.

$$\frac{c-c_1}{c_o-c_1}=\frac{8}{\pi^2}\sum_{n=0}^{\infty}\left(\frac{1}{(2n+1)^2}\left(\exp\left(-\frac{(2n+1)^2\pi^2}{4}\frac{Dt}{x^2}\right)\right)\right) \qquad (2.15)$$

Where:

c = average concentration at any time (kg/m^3)

c_0 = initial average concentration (kg/m^3)

c_1 = surface concentration = 0 (kg/m^3)

x = slab thickness (m)

D = moisture diffusion coefficient (m^2/s)

t = time (s)

Rice and Gamble (1989) assumed that the potato slice is an infinite slab and ignored the second and subsequent terms for long frying time (Fo > 2.0). A negligible surface resistance was assumed and relationship between apparent diffusion coefficient and temperature was also assumed to be an Arrhenius-type. The authors also related frying time, t (s) to the square of moisture loss (% initial weight).

$$m^2 = at + C \qquad (2.16)$$

Where the intercept (*C*) was linearly related to oil temperature *T (*°C) by the regression equation:

$$C = 40T - 6036 \qquad (2.17)$$

Semi empirical relationships were proposed for heat and mass transfer during frying of crustless and crust-forming products (Mittelman *et. al.,* 1984). The amount of water evaporated was found to be proportional to the square root of the frying time and the temperature difference between the oil and boiling water. For the crustless product, it was assumed that evaporation of water takes place from a receding front of liquid water at boiling temperature, the mass fraction of the solid matrix in the wet food is very low and that all the heat transferred from the oil to the food is used up in evaporation of water. The following equation was proposed:

$$m^2 = \frac{2kA^2\rho}{\lambda}(T_o - T_w)(t - t_o) \qquad (2.18)$$

For the crust-forming product, it was assumed that the temperature of the core remain constant at 100°C throughout the particle, the thickness of the crust remains constant throughout the latter stage of frying following the initial openings and cracks in the crust at the beginning of crust formation. The following equation was developed:

$$y^2 = C_2 \exp(0.0113T_{oil})(t - t_o) \qquad (2.19)$$

Where:

y = cumulative quantity of water evaporated (kg)

k = thermal conductivity (W/m°C)

A = area of heat and mass transfer (m^2)

ρ = density of the wet food (practically that of water) (kg/m^3)

λ = latent heat of evaporation of water (J/kg)

T_{oil} = temperature of the oil (°C)

T_w = boiling temperature of water (°C)

t = time (s)

t_o = time elapsed until evaporation starts (s)

C_2 = proportionality constant.

Farkas and co-workers (1996a, 1996b) developed a one-dimensional model for heat and moisture transfer during deep fat frying for material with infinite slab geometry and a moving boundary for the crust. Separate equations for the crust and the core regions were given as follow:

For heat transfer, core region:

$$k_{eff}^{II}\frac{\partial^2 T}{\partial x^2}+N_{\beta x}C_{p\beta}\frac{\partial T}{\partial x}=(\varepsilon_\beta\rho_\beta C_{p\beta}+\varepsilon_\sigma\rho_\sigma C_{p\sigma})\frac{\partial T}{\partial t} \qquad (2.20)$$

For heat transfer, crust region:

$$k_{eff}^{I}\frac{\partial^2 T}{\partial x^2}+N_{\gamma x}C_{p\gamma}\frac{\partial T}{\partial x}=(\varepsilon_\gamma\rho_\gamma C_{p\gamma}+\varepsilon_\sigma\rho_\sigma C_{p\sigma})\frac{\partial T}{\partial t} \qquad (2.21)$$

For mass transfer, core region:

$$\frac{\partial c_\beta}{\partial t}=D_{\beta\sigma}\frac{\partial^2 c_\beta}{\partial x^2} \qquad (2.22)$$

For mass transfer, crust region:

$$\frac{\partial}{\partial x}\left[\rho_\gamma\frac{\partial P_\gamma}{\partial x}\right]=0 \qquad (2.23)$$

Where:

k_{eff} = effective thermal conductivity (W/m.K)

T = temperature (°C)

ε_i = volume fraction of specie i (m_i^3 / m_t^3)

C_{pi} = specific heat of specie i (J/kg.K)

N_{ix} = flux of species i in x-direction ($kg / m_t^2 s$)

P = pressure (N/m^2)

t = time (s)

ρ_i = density of species i (kg / m_i^3)

c_β = concentration of β = $\varepsilon_\beta \rho_\beta$ (kgβ/ m_t^3)

D = mass diffusivity (m^2/s)

x = distance in the direction of heat or mass transfer

β, γ, σ are Liquid water, water vapour and solid phases respectively.

The partial differential equations were solved by a numerical method using coordinate transformation of the equations, application of the finite difference method of Crank-Nicholson and finally Gauss-Seidel iteration. The researchers assumed advection of energy due to oil flux is negligible and that the mass fraction of oil in the fried material is also negligible. The model did not include fat transfer. Pressure-driven flow was considered only for the vapor phase in the crust region. Both diffusional flow in the crust region and pressure-driven flow in the core region were ignored. One-dimensional models with boundary and initial conditions for moisture and heat transfer for a tortilla chip

during frying were derived with diffusion equation by Moreira *et. al.,* (1995a, 1995b), as follows:

Mass balance for moisture content of the product,

$$\frac{\partial m}{\partial t} = D\left[\frac{\partial^2 m}{\partial x^2}\right] \tag{2.24}$$

Energy Balance for the product,

$$\frac{\partial T}{\partial t} = \alpha\left[\frac{\partial^2 T}{\partial x^2}\right] \tag{2.25}$$

Moreira *et. al.* (1995a, 1995b) also described oil uptake as a function of the frying time by a first order exponential equation,

$$M_f(t) = M_{fe}\left[1 - \exp(-k't)\right] \tag{2.26}$$

Where:

m = moisture content (% d.b.)

D = mass diffusivity (m^2/s)

x = variable distance along thickness of tortilla chip (m)

M_f = oil content (%)

α = thermal diffusivity (m^2/s)

M_{fe} = final oil content (%)

k' = a constant (1/s)

t = time (s)

T = temperature (°C).

Negligible shrinkage and constant thermal and moisture diffusivities were assumed. No transport model for the oil phase was provided. The equations

were solved using explicit finite difference technique.

Atteba and Mittal (1994) used a one-dimensional model to describe heat, moisture and fat transfer for deep fat frying of beef meatballs. In the model, a general diffusion equation was used for heat transfer, moisture transfer and fat transfer in the absorption period. Capillary flow equation was used for fat transfer during desorption period. The models developed in non-dimensional form were:

For moisture transfer,

$$\frac{\partial C}{\partial t} = \frac{D_m}{R^2}\left(\frac{2}{\psi}\frac{\partial C}{\partial \psi} + \frac{\partial^2 C}{\partial \psi^2}\right); \quad (2.27)$$

For fat transfer (absorption),

$$\frac{\partial C_f}{\partial t} = \frac{D_f}{R^2}\left(\frac{2}{\psi}\frac{\partial C_f}{\partial \psi} + \frac{\partial^2 C_f}{\partial \psi^2}\right); \quad (2.28)$$

For heat transfer,

$$\frac{\partial \theta}{\partial t} = \frac{\alpha}{R^2}\left(\frac{2}{\psi}\frac{\partial \theta}{\partial \psi} + \frac{\partial^2 \theta}{\partial \psi^2}\right); \quad (2.29)$$

Where:

$$C = \frac{m - m_e}{m_o - m_e}; \quad (2.30)$$

$$C_f = \frac{mf - mf_e}{mf_o - mf_e}; \quad (2.31)$$

$$\theta = \frac{T - T_o}{T_a - T_o}; \quad (2.32)$$

$$\psi = \frac{r}{R}. \qquad (2.33)$$

For fat transfer (desorption),

$$V\frac{dmf}{dt} = -KLA[mf - mfep]; \qquad (2.34)$$

Where:

KL = fat conductivity (m/s)

V = product volume (m^3)

A = surface area (m^2)

mfep = equilibrium fat content (dry basis)

C = concentration

R = radius (m)

r = radial distance (m);

Ψ = dimensionless distance

α = thermal diffusivity (m^2/s)

D = mass diffusivity (m^2/s)

t = time (s)

T = temperature (°C)

θ = dimensionless temperature

m = moisture content (dry basis)

Subscripts *m, f, e, o, a* represent moisture, fat, equilibrium, initial and ambient respectively.

The equations were solved using finite difference technique. Fat and water were assumed to be mobilized by concentration gradients. The effect of

shrinkage and crust formation on physical properties of the product was also neglected. No evaporation term was included in the energy or moisture transport equations of this model except for the inclusion of surface evaporation as boundary condition for energy equation. The model was able to predict fat transfer during deep fat frying of a fatty product.

A multiphase porous media model was developed to simulate frying of potato slices (Ni and Datta, 1999). The model included the significance of pressure-driven flow for the oil, vapour and air phase in a non-hygroscopic porous medium. Five conservation equations for water vapour, liquid water, air, oil and energy in the porous medium were derived:

$$\frac{\partial c_v}{\partial t} + \nabla\left(\vec{n}_v\right) = \dot{I} \tag{2.35}$$

$$\frac{\partial c_w}{\partial t} + \nabla\left(\vec{n}_w\right) = -\dot{I} \tag{2.36}$$

$$\frac{\partial c_a}{\partial t} + \nabla\left(\vec{n}_a\right) = 0 \tag{2.37}$$

$$\frac{\partial c_o}{\partial t} + \nabla\left(\vec{n}_o\right) = 0 \tag{2.38}$$

$$\left(\rho c_p\right)_{eff} \frac{\partial T}{\partial t} = \nabla\left(k_{eff} \nabla T\right) - \lambda \dot{I} \tag{2.39}$$

Where:

$$\left(\rho c_p\right)_{eff} = \phi\left(S_g \rho_g c_{pg} + S_w \rho_w c_{pw} + S_o \rho_o c_{po}\right) + \left(1-\phi\right)\rho_s c_{ps} \tag{2.40}$$

$$k_{eff} = \phi\left(S_g k_g + S_w k_w + S_o k_o\right) + \left(1-\phi\right)k_s \tag{2.41}$$

c = mass concentration (kg/m^3)

n = total flux (kg/m^2.s)

t = time (s)

ϕ = porosity

ρ = density (kg/m^3)

P = pressure (Pa)

S = saturation

c_p = specific heat capacity (J/kg.K)

T = temperature (K)

$\dot{I}$ = volumetric expansion (kg/m^3.s)

k = thermal conductivity (W/m.K);

λ = latent heat of vaporization (J/kg).

Subscripts: *v, w, a, o, g, s, p, eff* are vapour, water, air, oil, gas (vapour+air), solid matrix (surface), partial pressure, and effective, respectively.

The five governing equations were transformed into four equations with variables S_w, S_o, *T and P* and were solved with a central finite difference method with initial and boundary conditions. Ni and Datta (1999) assumed the existence of thermal equilibrium between phases and ignored the contribution of convection to energy transport. The model was able to consider the transport of oil, water, vapour and air components separately. However, the model did not account for changes in porosity and its effect on energy and mass transport.

2.5 Heat and Mass Transfer Analogy

In deep fat frying, heat and mass transfer occur simultaneously. Even though researchers tend to separate the two processes for the purpose of

analysis, a complete analysis of one cannot be done without the other. A host of scientists has been involved in the historic development of the idea that a similar phenomenon guides both heat and mass transfer. Attempts have also been made to estimate one transport property (e.g. *D*) from another (e.g. *k*) as found in the Lewis equation.

Reynolds' analogy is probably the earliest known of heat and mass transfer analogies. Reynolds argued that under certain conditions, heat, mass and momentum transfer occur at the same rate (Incropera and Dewitt, 2004). The logic for this was that each of these transfer processes involves:

(1) natural diffusion in a fluid at rest; and

(2) eddies which bring fresh fluid into contact with a surface and allows transfer of specie to the surface.

While the former is independent of velocity, it is obvious that the latter is not. So, for turbulent flow, which is typical of frying, a mass flux can be calculated from:

$$n = h_m \Delta C = (a + bU)\Delta C \qquad (2.42)$$

Similarly, a heat flux can be expressed as:

$$q = h\Delta T = (a + b\,U)\Delta(\rho C_p T) \qquad (2.43)$$

Where:

n = mass flux (kg/m^2)

h_m = mass transfer coefficient (kg/m^2.s)

C = concentration of species (kg)

U = velocity (m/s^2)

q = heat flux (W/m^2)

h = heat transfer coefficient (W/m^2.K)

T = temperature (°C)

ρ = intrinsic density (kg/m^3)

C_p = specific heat capacity (J/kg.K).

a, a', b and *b'* are constants

For very turbulent flow, it is assumed that $a = a' = 0$, *i.e.* turbulent effects dominate. At this point, Reynolds also assumed that heat and mass transports were arising from the same turbulent mechanism and therefore assumed that $b = b'$. It follows then that the transport properties simplify to:

$$h_m = bU \tag{2.44}$$

$$\frac{h}{\rho C_p} = b'U \tag{2.45}$$

And since $b = b'$, then

$$\frac{h_m}{U} = \frac{h}{\rho C_p U} \tag{2.46}$$

Where:

h_m = mass transfer coefficient (kg/m^2.s)

h = heat transfer coefficient (W/m^2°C)

U = velocity (m/s)

ρ = density (kg/m^3)

C_p = heat capacity (J/kg.K)

The benefit of this work is that we can derive one transfer coefficient if we know the other. The Reynolds' analogy is true for gases but not for liquids. This

is better understood by recognizing that turbulent flow takes place at two levels: at an eddy level (macroscopic) and at a diffusional level (microscopic). The latter is buried in *b, b′* since Reynolds assume *a* = *a′* = 0. For gases, the diffusional level is expressed by $D \cong \alpha \cong \nu \cong 0.1\ m^2/s$. Or in a better sense: $\nu/D \cong \nu/\alpha \cong 1$, *i.e.* Sc = Pr. Which makes the analogy sensible.

For liquids, however, Sc and Pr are about 1000 and 10 respectively. (Sc = $\mu/(\rho D)$ and Pr = $C_p \mu/k$). These are definitely not the same and it invalidates the analogy for liquids.

Where

D = mass diffusivity (m^2/s)

v = kinematic viscosity (m^2/s)

α = thermal diffusivity (m^2/s)

Pr = Prandtl number (dimensionless)

Sc = Schmidt number (dimensionless)

k = thermal conductivity (W/m.K)

μ = dynamic viscosity (kg/m.s)

Reynolds ignored the laminar boundary layer in his work and a couple of scientists Taylor and Prandtl working with Reynolds analogy broke the flow into two regions: a laminar layer and a fully turbulent layer (Brodkey and Hershey, 1988). Using Fourier's and Newton's laws across the sub-layer, they developed a correction factor as below:

$$\frac{h}{C_p \rho U}(1+\alpha(\mathrm{Pr}-1)) = \frac{h_m}{U}(1+\alpha(Sc-1)) \qquad (2.47)$$

It can be seen from the result that for a very turbulent flow such that the boundary layer approaches zero (α = 0), then 1/(1+α(Pr-1)) approaches unity and this result approaches Reynolds analogy.

Chilton-Colburn analogy is an attempt to extend the Reynolds' analogy to liquids. It is purely empirical in basis. Chilton-Colburn decided that the basic form of the Reynolds' analogy was good, but that the b's should be replaced as follows:

$$b' = \frac{h}{\rho C_p U}\left(\frac{\nu}{\alpha}\right)^{\frac{2}{3}} \qquad (2.48)$$

$$b = \frac{h_m}{U}\left(\frac{\nu}{D}\right)^{\frac{2}{3}} \qquad (2.49)$$

Such that;

$$\frac{h_m}{U}\left(\frac{\nu}{D}\right)^{\frac{2}{3}} = \frac{h}{\rho C_p U}\left(\frac{\nu}{\alpha}\right)^{\frac{2}{3}} \qquad (2.50)$$

Once again, with the knowledge of one transfer coefficient, the other can be calculated from this equation. Due to the reason stated earlier regarding variation in Schmidt and Prandtl number for liquids, it is difficult to apply these results to frying. The best approach for now therefore is still empirical correlation using experimental results. The disadvantage of this approach is that the models developed are most suited only to products with similar geometry, physical properties and frying process requirements as the one used in developing the model.

2.6 Summary

Literature shows sweetpotato is an important crop. A lot of studies have been conducted on deep fat frying. Most of the works focused on heat transfer during frying, mechanisms and rate of moisture loss and fat uptake, quality kinetics of the fried food and the frying medium and mathematical modeling of the frying process. However information on thermal properties and deep fat frying of sweetpotato is lacking in literature. Also no work has been reported on heat and mass transfer analogy during deep fat frying.

3. MATERIALS AND METHODS

This chapter presents the materials used in this study and the methods that were used in conducting experiments or estimating properties values.

3.1 Materials

Sunny II sweetpotatoes (*Ipomoea batatas*) were bought in 20 kg lots from Eastern Market, (Saskatoon, SK) to avoid variability in quality and product chemistry. The potatoes were stored in a cooling chamber at a temperature range of 11±1°C usually for 24 h before use. The tubers were manually peeled with a hand peeler and then cut into discs using a cylindrical cutter and a knife. Samples were cut into discs having diameters of 2.5 cm, 3.5 cm and 4.0 cm, all with 1 ± 0.1 cm thickness. Canola oil (Sunnyfresh Ltd, Toronto, ON) was used as the frying oil in this study.

3.2 Density Measurement

Density of a material is the ratio of its mass to the volume it occupies. Two methods: Gas multipycnometer and a mechanistic model developed by Choi and Okos (1985) were used in this study.

3.2.1 Multipycnometer

Density of sweetpotato was measured at four different levels of moisture content 0.45, 0.55, 0.65, 0.75 w.b. Moisture content of sweetpotato was adjusted by heating the sample in a microwave oven (Panasonic NN-5553C, Matsushita Corporation, Franklin Park, IL). The oven had been previously calibrated to determine the heating time to get sample to a desired moisture content level. The microwave oven initially has been calibrated at a constant power (800 W) to determine the heating time required to dry sample to the required moisture content. After heating, the sample was equilibrated for 6 h and the moisture content was determined by oven method of AOAC standard 984.25 (AOAC, 2002) to check if the moisture content is of the expected value.

Density of sweetpotato was determined in 5 replicates using the multipycnometer (Quantachrome Corporation, Boynton Beach, FL). The instrument is shown in Figure 3.1. It measures the true volume of a solid material. It makes use of two cylindrical volumes; reference volume which is empty and the other volume containing the sample. The instrument makes use of a displacement fluid with very small atomic dimension to penetrate the pores of the material.

Figure 3.1: Multipycnometer used to measure density of sweetpotato.

The volume of the sample is given by the equation:

$$V_P = V_C - V_R\left[\left(\frac{P_1}{P_2}\right) - 1\right] \qquad (3.1)$$

Where:

V_p = volume of the sample (cm^3);

V_c = volume of the cell containing the sample (cm^3);

V_R = volume of the reference cell (cm^3);

P_1 = pressure reading after pressurizing the reference volume (psi); and

P_2 = pressure reading after including V_c (psi).

True density of the sample was then determined from the ratio of sample mass to its volume determined above.

$$\rho = \frac{m}{V_P} \qquad (3.2)$$

Where:

ρ = density (kg/m^3)

V_P = volume of sample (m^3) as determined from multipycnometer

m = mass (kg).

Sample mass was determined by weighing the sample on an Ohaus GA2000 balance (Ohaus Corp., Pine Brook, NJ). Multipycnometer was calibrated before use as suggested in the manual to ensure that a correct value for the reference volume was used. A regression model was developed with SAS (SAS Institute Cary, NC) for the density result from this experiment as a function of moisture content.

3.2.2 Mechanistic Model

Choi and Okos (1985) developed models for thermal properties of food products. Models were developed for estimating properties like density, specific heat capacity, thermal conductivity and thermal diffusivity of major components of food: carbohydrate, fat, protein, ash, fibre and water. Percentage composition of these major components in sweetpotato was derived from USDA agricultural handbook (USDA, 1963). Choi and Okos (1985) have demonstrated that thermal properties of food materials are dependent on composition of major food components in the particular food. Variation of these major food components among different samples of a food variety is negligible. The models give very accurate predictions for a wide range of food materials. Also, solid components

were shown to have lesser influence than that of water on the thermal properties of the food. It was on this basis that the developed mechanistic models for major food components (Choi and Okos, 1985) and food composition data for sweetpotato (USDA, 1963) were used in this study.

The models were developed as a function of temperature and are presented in Table 3.1. Percentage composition of major food components in sweetpotato is presented in Table 3.2. The particular property for a food product is then estimated by combining the results of models in Table 3.1 with mass fraction (specific heat and density) or volume fraction (thermal conductivity and thermal diffusivity) of each component using series or parallel models. The model for density (equation 3.3) was used in this study to estimate the density of sweetpotato both as a function of temperature and moisture content. Based on the chemical composition of sweetpotato, Excel (Microsoft Corp. Redmond WA) was used to generate density with moisture content range of 0.45-0.75 w.b. and temperature range of 20-150°C. The series model was chosen over the parallel model for estimating density because density variation among major food components is wide. Density of water and fat are different from densities of other components. The series model predicts a better value in such circumstances (Stroshine, 1998). A regression equation was developed for the data.

Table 3.1. Models of thermal properties and density of major components of foods. (adapted from Choi and Okos, 1985).

Thermal Property	Major component	Group models temperature function	Standard error	Standard % error
	Protein	$k = 1.7881 \times 10^{-1} + 1.1958 \times 10^{-3}T - 2.7178 \times 10^{-6}T^2$	0.012	5.91
	Fat	$k = 1.8071 \times 10^{-1} - 2.7604 \times 10^{-3}T - 1.7749 \times 10\text{-}'T^2$	0.0032	1.95
k	Carbohydrate	$k = 2.0141 \times 10^{-1} + 1.3874 \times 10^{-3}T - 4.3312 \times 10^{-6}T^2$	0.0134	5.42
W/m°C	Fiber	$k = 1.8331 \times 10^{-1} + 1.2497 \times 10^{-3}T - 3.168\ 3 \times 10^{-6}T^2$	0.0127	5.55
	Ash	$k = 3.2962 \times 10^{-1} + 1.4011 \times 10^{-3}T - 2.906\ 9 \times 10^{-6}T^2$	0.0083	2.15
	Protein	$\alpha = 6.8714 \times 10^{-2} + 4.7578 \times 10^{-4}T - 1.4646 \times 10^{-6}\ T^2$	0.0038	4.50
	Fat	$\alpha = 9.8777 \times 10^{-2} - 1.2569 \times 10^{-4}T - 3.8286 \times 10^{-8}T^2$	0.0020	2.15
α	Carbohydrate	$\alpha = 8.0842 \times 10^{-2} + 5.3052 \times 10^{-4}T - 2.3218 \times 10^{-6}T^2$	0.0058	5.84
m^2/s	Fiber	$\alpha = 7.3976 \times 10^{-2} + 5.1902 \times 10^{-4}T - 2.2202 \times 10^{-6}T^2$	0.0026	3.14
	Ash	$\alpha = 1.2461 \times 10^{-1} + 3.7321 \times 10^{-4}T - 1.2244 \times 10^{-6}T^2$	0.0022	1.6
	Protein	$\rho = 1.3299 \times 10^{3} - 5.1840 \times 10^{-1}T$	39.9501	3.07
	Fat	$\rho = 9.2559 \times 10^{2} - 4.1757 \times 10^{-1}T$	4.2554	0.47
ρ	Carbohydrate	$\rho = 1.5991 \times 10^{3} - 3.1046 \times 10^{-1}T$	93.1249	5.98
kg/m^3	Fiber	$\rho = 1.3115 \times 10^{3} - 3.6589 \times 10^{-1}T$	8.2687	0.64
	Ash	$\rho = 2.4238 \times 10^{3} - 2.8063 \times l0^{-l}T$	2.2315	0.09
	Protein	$C_p = 2.0082 + 1.2089 \times 10^{-3}T - 1.3129 \times 10^{-6}T^2$	0.1147	5.57
	Fat	$C_p = 1.9842 + 1.4733 \times 10^{-3}T - 4.8008 \times 10^{-6}T^2$	0.0236	1.16
Cp	Carbohydrate	$C_p = 1.5488 + 1.9625 \times 10^{-3}T - 5.9399 \times 10^{-6}T^2$	0.0986	5.96
kJ/kg.K	Fiber	$C_p = 1.8459 + 1.8306 \times 10^{-3}T - 4.650\ 9 \times 10^{-6}T^2$	0.0293	1.66
	Ash	$C_p = 1.0926 + 1.8896 \times 10^{-3}T - 3.6817 \times 10^{-6}T^2$	0.0296	2.47

Table 3.2. Percentage composition of major food components in sweetpotato (adapted from USDA, 1963)

Component	Percentage by mass (%)
Protein	1.7
Fat	0.4
Carbohydrate	26.3
Fibre	0.7
Ash	1.0
Water	69.9

$$\rho = \frac{1}{\sum \frac{X_i^w}{\rho_i}} \tag{3.3}$$

Where:

X_i^w = weight fraction of component I (kg)

ρ_i = density of pure component I (kg/m^3).

ρ = density of sweetpotato (kg/m^3)

3.3 Specific heat

Specific heat capacity, C_p is defined as the amount of heat needed to raise the temperature of 1 kg of a material by 1 degree K. It depends mainly on the composition of the material, temperature and pressure. C_p also decreases with a decrease in moisture content. Specific heat capacity for this study was determined both from mechanistic models and experimentally using a differential scanning calorimetry (DSC). Specific heat capacity was determined as a

function of product temperature (20-180°C) and moisture content (0.45, 0.55, 0.65, 0.75 (w.b)).

3.3.1 Mechanistic model

Specific heat of sweetpotato was estimated as a function of temperature and moisture content based on the mass fraction of the components using Excel. The parallel model (equation 3.4) was used since it applies better to non-fibrous materials where thermal properties are not dependent on direction of heat flow and variation in C_p of major food components is not large (Stroshine, 1998). A regression equation was then developed for the generated data using SAS (SAS Institute, Cary NC).

$$C_p = \sum C_{pi} X_i^w \qquad (3.4)$$

Where:

X_i^w = weight fraction of component i

C_{pi} = specific heat of pure component i (J/kg.K)

C_p = specific heat of sweetpotato (J/kg.K)

3.3.2 Differential Scanning Calorimeter

DSC method is very popular in determining specific heat of food materials. The technique is direct, relatively quick and dynamic over a wide range of temperature. However, it is expensive, requires calibration since it is a comparative device, and requires only a very small product sample which might make it difficult to obtain homogenous samples that are truly representative of

the product.

3.3.2.1 Sample preparation

Sweetpotato samples to be run on DSC were prepared by peeling and cutting the tuber into tiny pieces of approximately 2 × 2 × 2 mm by surgical blade. This was by no means precision cutting. The aim was just to have tiny pieces small enough such that a few pieces would give a mass of about 10-12g required for the experiment and fit into the sample pan. The sample was then heated in a microwave oven to get it to desired moisture content. Samples for this experiment were at four moisture content values of 0.45, 0.55, 0.65 and 0.75 wet bases. The microwave oven initially has been calibrated at a constant power to determine the heating time required to dry sample to the required moisture content. After heating, the sample was equilibrated for 6 h and the moisture content was determined by oven method of AOAC standard 984.25 (AOAC, 2002) to check if the moisture content is of the expected value.

3.3.2.2 Experimental procedure

Differential scanning calorimeter (DSC) shown in Figure 3.2 was also used in determining the specific heat of sweetpotato. The model is DSC 2010 (TA Instrument Inc., New Castle, DE). The DSC includes a holder housing two discs which are in thermal contact with each other and are isolated from the environment. Two sample pans were prepared; one of the pans contained the sample to be measured while the other was an empty reference pan. The sample pan contained 10-12 mg of the sample. This was hermetically sealed.

The pans were placed on the discs in the holder and the holder was closed. The discs sat on a raised platform on a constantan disc. Both pans were heated at a controlled, known heating rate of 10°C/min. in this case and the heat flow between the pans, which gives the difference in heat capacity of the reference pan and the sample, was monitored by thermocouples beneath the disc and measured. Specific heat of the sample is estimated from the heat flow rate, heating rate and the mass of the sample (equation 3.5). The experiment was carried out in duplicates. The DSC is a comparative device and must be calibrated. Prior to use, the DSC was calibrated with water. The data analysis software used was TA Universal Analysis (TA Instruments, New Castle, DE). The operational equation of the software is as shown in equation (3.5)

Figure 3.2: DSC 2010 used for specific heat measurement of sweetpotato.

$$C_p = \frac{dQ/dt}{mdT/dt} \qquad (3.5)$$

Where:

C_p = heat capacity (J/g.K)

dQ/dt = heat flow rate (J/s)

dT/dt = heating rate (K/s)

m = mass of the sample (g)

Often during the experiment there was leakage (most especially at very high temperatures) in which moisture vapour escaped from the sample pan. This is due to increased vapour pressure as heating progresses, if the pans were not sealed properly. It is therefore important that the pan is properly sealed to avoid moisture vapour loss during heating. Some of the runs in this study leaked and they were repeated.

3.4 Thermal Conductivity

Thermal conductivity, *k* gives the rate at which heat is conducted through a unit thickness of a material when a unit temperature gradient exists across the thickness. From Fourier equation, heat flow in the material is given by:

$$q = -k\frac{\partial T}{\partial x} \qquad (3.6)$$

Where

q = heat flow (W)

k = thermal conductivity (W/m.K)

∂T = change in temperature (K)

∂x = material thickness (m)

It is a function of heat flow, area perpendicular to its direction and temperature drop in a sample. For a porous media consisting of solid and gas phases, the measured thermal conductivity is an apparent one, usually called the effective thermal conductivity (k_{eff}). It is an overall transport property assuming that heat is transferred by conduction through the solid and the porous phase.

Thermal conductivity in this study was determined with mechanistic models of food major components using the work of Choi and Okos (1985) as outlined in Table 3.1. Thermal conductivity of sweetpotato was then estimated from these models as a function of temperature and moisture content based on the volume fraction of the components (equation 2.6) using Excel. The parallel model was chosen over the series model to determine thermal conductivity since thermal conductivity in vegetables are not dependent on the direction of heat flow as it is in fibrous materials like fish and meat. Also, variation among *k* of major food components is not large (Stroshine, 1998). Result from parallel model also compare better with values in literature. A regression equation was also developed for the generated data using SAS.

An attempt was made at determining thermal conductivity experimentally using both the line heat source method and KD2 thermal properties analyzer (Decagon Devices Inc. Pullman, WA). However, there was significant error in the results in particular at temperature beyond boiling point (100°C) for the line heat source method. Some line heat source methods can handle higher temperature than 100°C, however it would cause significant deviation due to condensation and moisture loss at higher temperature. Since frying is done at

temperature range of 150-170°C, this questions the ability of the line heat source method to determine thermal conductivity at typical frying temperature. For the KD2 thermal properties analyzer, its operating temperature is limited to 60°C. This limits its use for studying thermal properties for frying application.

3.5 Thermal diffusivity

Thermal diffusivity is the rate at which heat diffuses through a material. The property is needed in establishing a temperature history of a body under transient condition from Fourier's law of heat conduction. Thermal diffusivity of sweetpotato in this study was determined with thermal diffusivity models of food major components using the work of Choi and Okos (1985) shown in Table 3.1. Thermal diffusivity estimation was based on volume fraction of the components (equation 3.7). A regression equation was also developed for the generated data using SAS.

$$\alpha = \sum \alpha_i X_i^v \qquad (3.7)$$

Where:

X_i^v = volume fraction of component i (m^3)

α_i = thermal diffusivity of component i (m^2/s)

α = thermal diffusivity of sweetpotato (m^2/s).

3.6 Moisture diffusivity

Moisture diffusivity, *D* is the rate at which moisture diffuses through a material. Most of the available methods of determining diffusivity are based on

Fick's laws of diffusion. D in this study was estimated from the relationship in equation (3.8)

$$D = \frac{k_m}{\rho C_m} \qquad (3.8)$$

Where:

D = moisture diffusivity (m^2/s)

k_m = moisture conductivity ($kg_{moisture}/m.s$)

ρ = density of sample (kg/m^3)

C_m = specific moisture capacity ($kg_{moisture}/kg_{sample}$)

k_m and C_m were derived from literature (Sheerlinck *et.al.,* 1996; Chen *et.al.,* 1999). Density was experimentally determined as described under section 3.2. Since k_m and C_m are constants and density was modeled as a function of moisture content only, moisture diffusivity variation with frying condition is limited to change in moisture content only. A model that includes the effect of temperature would however have been more accurate in predicting mass transfer rate.

3.7 Deep fat frying

This is the actual cooking of the sweetpotato in oil. It is usually done at a temperature above the boiling point of water typically 150-190°C.

3.7.1 Sample preparation

Sweetpotato tubers were peeled with a hand peeler and then cut into discs using a cylindrical borer and a knife. Samples were cut into discs having diameters 2.5 cm, 3.5 cm and 4.0 cm, all with 1 ± 0.1 cm thickness (Figure 3.3).

Figure 3.3: Sweetpotato sample sizes and cylindrical borers used to cut samples.

3.7.2 Sample holder

Frying is a very turbulent process in which the product moves around randomly in the oil. One of the major challenges of studying the process is in making the product stable enough so as to be able to measure its temperature. For this study, a sample holder (Figure 3.4) was designed and fabricated. It essentially has a handle made of Teflon which holds the product and the steel frame that ensures product's stability in the turbulent oil. One of the handles was adjustable such that the holder can handle multiple sizes. Three holes were

bored into the other handle to accommodate thermal probes which measure the temperature within the sample (Figure 3.4). Making the arm of a poor conductor of heat like Teflon ensures heat conduction to sample is limited to oil only and does not involve heating from the sample holder arm.

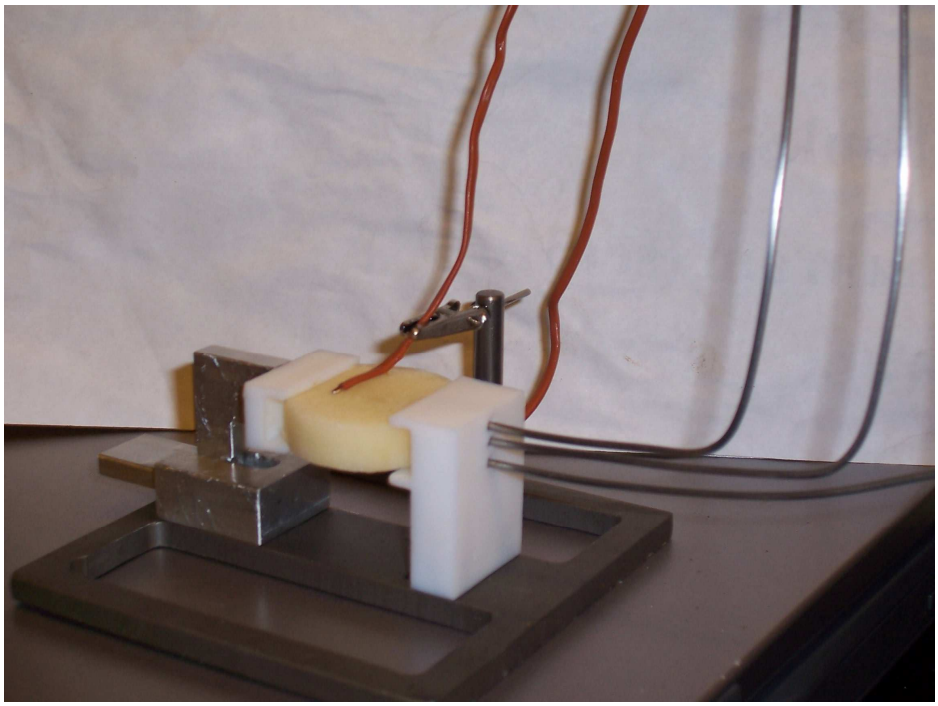

Figure 3.4: Sample holder used for frying with thermocouples attached.

3.7.3 Experimental procedure

A domestic deep-fryer (Cool Touch deep fryer, General Electric, Mississauga, ON) shown in Figure 3.5 was used for this study. The fryer has a power rating of 1500W, frying volume capacity of 2 litres and regulates frying temperature to ±1°C. The fryer has a built-in thermostat for oil temperature regulation. It also has a temperature indicator but a type-*K* thermocouple was also used to measure oil temperature during frying. The sample disc was fixed inside the sample holder and the sample holder was adjusted with a tight-screw

to ensure sample was tightly held. Three thermal probes made from type-*T* thermocouple were inserted into the sample through the holes in the fixed arm of the holder and two other type-*T* thermocouple were tightly pressed to the surface of the product by a couple of alligator clips built into the sample holder (Figure 3.4).

Two litres of canola oil was poured into the deep fryer up to the maximum mark. Fryer was switched on and its temperature was set to the desired level (150, 160, 170 or 180°C). After the oil temperature has reached the desired level as indicated by the fryer indicator and the thermocouple, the sample holder with the sample in it was lifted with a long holder and placed inside the fryer (Figure 3.6). The sample was kept in the frying oil for the required frying time which was typically 300 s. A timer was used to regulate the frying period. The sample was then removed from the oil with the same long holder after the desired frying time. The thermocouples, most especially the ones on the surface were checked after each frying period to make sure that they were still in place and measuring the right temperature. Data from experiments in which the surface thermocouples were found to be embedded in the sample crust or found separated from the surface were discarded. Four frying temperatures of 150, 160, 170 and 180°C were used in this study. Also, three sample sizes having diameters 2.5 cm, 3.5 cm and 4.0 cm, all with 1 ± 0.1 cm thickness were used.

Figure 3.5: Deep fryer used for sweetpotato frying.

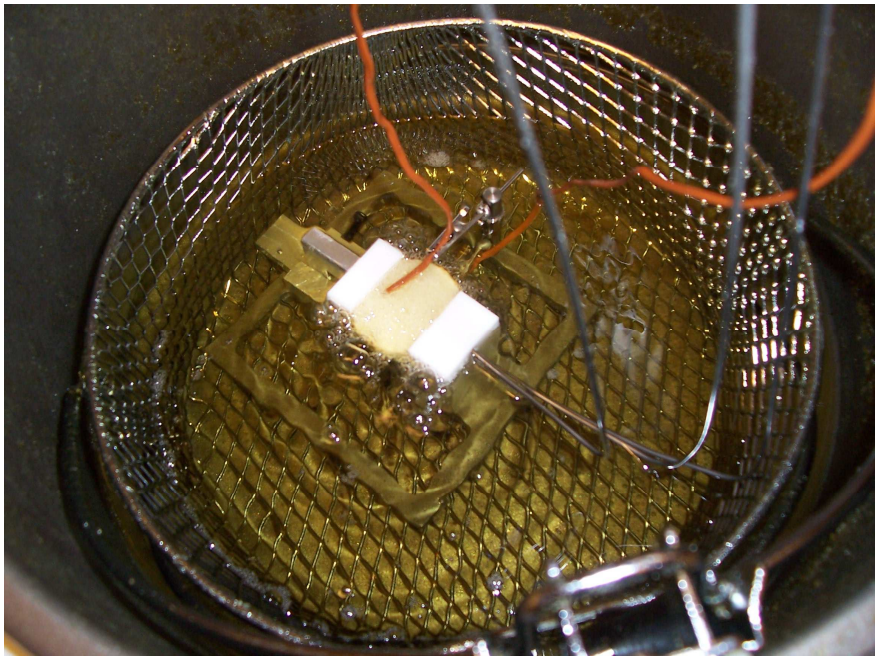

Figure 3.6: Sweetpotato sample in the oil during frying.

3.7.4 Temperature measurement

A CR10X datalogger (Campbell Scientific Instrument, Logan UT) was used to acquire real time temperature data in this study. Three type-T thermal probes were used to measure temperature inside the sample while 2 type-*T* thermocouples were used to measure the surface temperature of the sample. The 5 thermocouples were connected to the datalogger and the datalogger was programmed to obtain temperature data from the sample.

3.7.5 Moisture content measurement

Moisture content was measured in the crust and core parts of the fried sample and the raw whole sweetpotato sample. Moisture content during frying was measured at seven time intervals (0, 30, 60, 120, 180, 240 and 300 s) using the oven method according to AOAC Method 984.25 (AOAC, 2002). Frying was done for each specific time interval enumerated above; the product was then removed from the oil and oil on the surface was dried using a blotting paper. For the measurement of moisture content of whole sample, the sample was cut into smaller pieces using a surgical knife as mentioned under section 3.3.2.1, weighed on a mass balance (Ohaus GA2000, Ohaus Corp. PineBrook, NJ) and then dried in the oven (Blue M, General Signal, Blue Island, IL) at 103ºC for 48 h and moisture content was determined using the AOAC official method stated under section 3.3.2.1.

For crust and core part moisture content determination, a surgical blade was used to carefully remove the core from the crust (Figure 3.7). The part of interest was then weighed and oven dried to determine the moisture content.

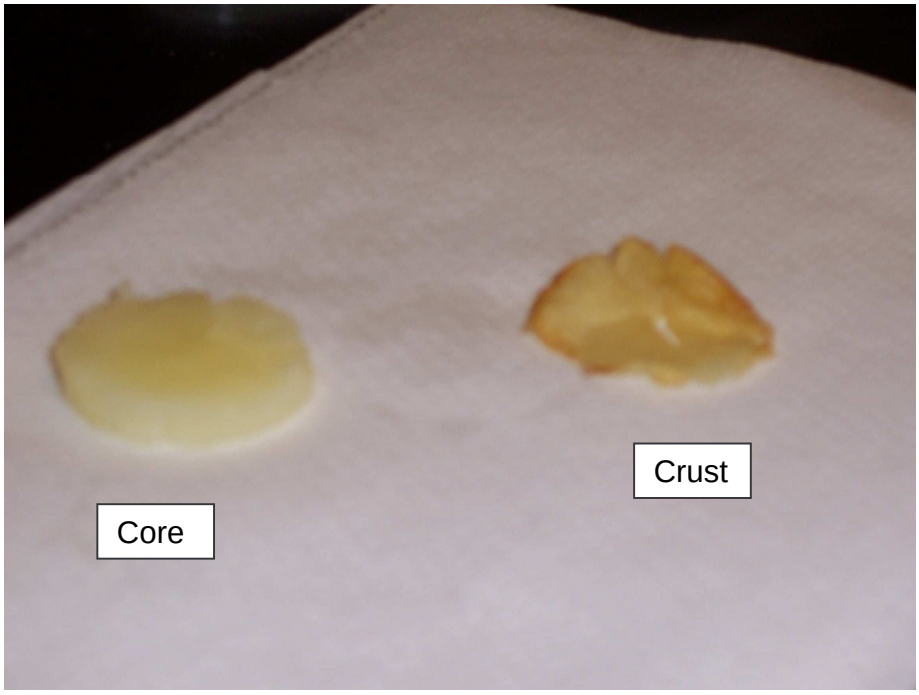

Figure 3.7: Crust and core samples of sweetpotato after frying.

3.8 Heat transfer coefficient

The rate of heat transfer from the oil to the sweetpotato is controlled by the convective heat transfer coefficient, *h* at the boundary between the food and the oil. The heat transfer coefficient, in this study, was estimated from the heat energy balance during frying. The energy balance during frying equates total heat transferred by convection from oil to sweetpotato to the sum of energy spent on heating sweet potato and energy spent on water evaporation. This is represented by equation (3.9).

$$hA\left(T_{\infty} - T_{s}\right) = MC_{p}\frac{dT}{dt} + \lambda\frac{dm}{dt} \qquad (3.9)$$

Where:

h = heat transfer coefficient (W/m^2°C)

A = area (m^2)

T_∞ = oil temperature (°C)

T_s = sweetpotato's surface temperature (°C)

M = mass of sweetpotato sample (kg)

C_p = specific heat capacity (J/kg°C)

T = volume temperature of sweetpotato (°C)

t = time (s)

m = moisture content of sweetpotato (kg)

λ = latent heat of evaporation (J/kg)

The frying time (300 s) was divided into 6 periods and average heat transfer coefficient, h of sweetpotato was calculated for each of these periods using equation (3.9). A mathematical expression previously developed for specific heat capacity of sweetpotato as a function of temperature and moisture content was substituted in equation (3.9) towards determining h. Volume average temperature was determined by numerical integration of temperature data at 5 different locations in the sample.

3.9 Computer simulation of heat and mass transfer

This section discusses the method adopted for computer simulation of heat and moisture transfer in sweetpotato during frying.

3.9.1 COMSOL™ software

Mass transfer coefficient, h_m of sweet potato during frying was

determined using a computer simulation software (COMSOL™ Multiphysics, COMSOL Inc. Los Angeles, CA). COMSOL™ is a PDE-based multiphysics tool that makes use of finite element modeling (FEM). In FEM, a domain defining a continuum is discretized into simple geometric shapes called elements (Figure 3.8). Properties and the governing relationships are assumed over these elements and expressed mathematically in terms of unknown values at specific points in the elements called *nodes*. The elements in the domain are linked by an assembly process. Solution of the governing equations of the phenomenon, initial conditions and boundary conditions in the domain gives the approximate predict

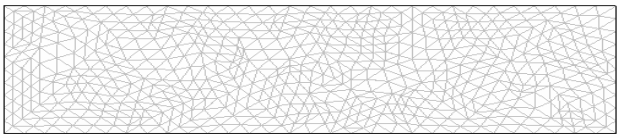

Figure 3.8: Mesh generation in the sweetpotato sample domain.

COMSOL™ has a host of built-in specialized modules for a field-specific problems. COMSOL™ also has the capability of creating personal equation-based models by the user. All these can be achieved through the use of the software's graphical user interface (GUI) or through the MATLAB™ (The Mathworks Inc. Natick, MA) prompt.

3.9.2 Backgrounds, assumptions and approach to simulation

Two different phenomena, heat transfer and mass transfer were coupled in this mathematical modeling. Both of the phenomena have an effect on each other and occur simultaneously during frying. Due to the symmetrical nature of the sweetpotato sample discs (Figure 3.9), simulation was done in 2-dimension with the following assumptions:

1. initial temperature and moisture content distribution in sweetpotato is uniform;
2. the temperature and moisture content fields on the inner boundaries are symmetrical;
3. the product is homogeneous and isotropic;
4. product shrinkage during frying is negligible;
5. crust was assumed to be negligible and have same properties as whole sample;
6. moisture movement is by diffusion and moisture diffusivity encompasses other mechanisms including convection; and
7. a microscopically uniform porous medium was formed after frying and most oil diffuses into the product during the cooling period.

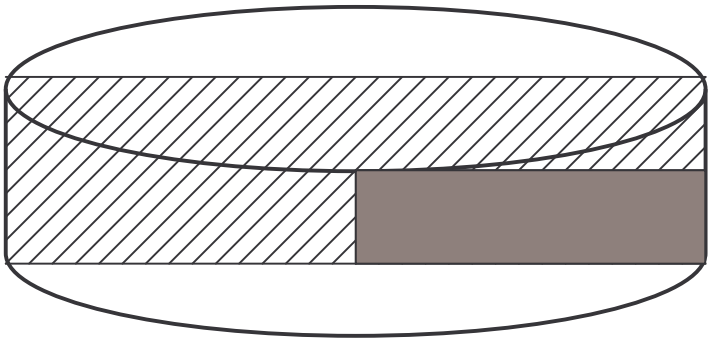

Figure 3.9: Sweetpotato sample disc geometry.

The input data for this simulation were the thermal and physical properties models of sweetpotato (density, thermal conductivity, specific heat, moisture diffusivity, heat transfer coefficient and latent heat of evaporation of moisture) along with experimental parameters like oil temperature, initial product temperature of sample and physical model of sample. Latent heat of evaporation for moisture was assumed constant for temperature above 100°C and taken to be 2.257×10^6 J/kg (Incropera and Dewitt, 1994).

Heat transfer coefficient of sweetpotato determined under section 3.8 was an input into the model in interpolation form as a function of time. A guess value for mass transfer coefficient, h_m was then an input in a time-defined interpolation form for the first time step (0-30 s of frying) and process is simulated. Temperature profile of the sample (product surface and center) and moisture content profile (surface and whole sample) were extracted and compared to experimental data under the same set of conditions. h_m was adjusted appropriately until the best fit was obtained between temperature and moisture content data from simulation and experiment. The simulation process is then

repeated for the next time step of 30-60 s of frying while keeping the h_m from the last step (0 - 30 s) as an input for the previous step to guide the present step. This process was repeated until h_m for the last time step (240–300 s) was obtained, each time comparing data (temperature and moisture content) from the simulation to experimental data to obtain h_m that gives the best fit.

3.9.3 Criterion for best fit

In the simulation, two temperatures (sample surface temperature, T_s and center temperature, T_c were compared for both experiment and simulation. Also compared were moisture content of the surface, M_s and that of the centre, M_c for experiment and simulation. The goal was to minimize the deviation between experimental data and simulation data and this was done using the root square deviation of normalized temperature and moisture content data. Best h_m data was adopted from the one that gives the least value of Dev. As given in equation 3.10.

$$Dev = \sqrt{\sum_{i=1}^{n}\left(\left(\frac{T_{ci,measured} - T_{ci,simulated}}{T_{ci,measured}}\right)^2 + \left(\frac{T_{si,measured} - T_{si,simulated}}{T_{si,measured}}\right)^2 + \left(\frac{M_{ci,measured} - M_{c,simulated}}{M_{ci,measured}}\right)^2 + \left(\frac{M_{s,measured} - M_{s,simulated}}{M_{si,simulated}}\right)^2\right) \Big/ n} \qquad (3.10)$$

3.9.4 Governing equations, initial conditions and boundary conditions

Computer simulation of frying was done with COMSOL™ multiphysics using governing equations for heat and mass transfer with initial and boundary conditions on a domain representing the product.

3.9.4.1 Governing equations

The governing differential equation describing temperature change in the sweetpotato disc during frying is described in equation (3.11) (Incropera and Dewitt, 1994; Moriera *et. al.,* 1999). The first term on the left represents axial spatial temperature change in the domain, the second term on the left represent radial spatial temperature change in the domain, the third term on the left represent the heat transfer caused by diffusion of water vapour where Γ is the water vapour flux. The right hand term represents temperature change with time.

$$\frac{\partial}{\partial x}\left(k\frac{\partial T}{\partial x}\right)+\frac{1}{r}\frac{\partial}{\partial r}\left(kr\frac{\partial T}{\partial r}\right)-\frac{\partial\left(\Gamma C_{pw}T\right)}{\partial x}=\frac{\partial\left(\rho C_{p}T\right)}{\partial t} \qquad (3.11)$$

$$\Gamma=-\frac{\partial\left(\rho DM\right)}{\partial x} \qquad (3.12)$$

Equation (3.13) describes moisture transfer during frying. The left hand term represents spatial moisture content change in the domain while the right hand term represents moisture change with time.

$$\frac{\partial}{\partial x}\left(D\rho\frac{\partial M}{\partial x}\right)+\frac{1}{r}\frac{\partial}{\partial r}\left(D\rho r\frac{\partial M}{\partial r}\right)=\frac{\partial\left(\rho M\right)}{\partial t} \qquad (3.13)$$

3.9.4.2 Initial and boundary conditions

Initial conditions: Temperature and moisture content within the sweetpotato sample prior to frying are uniform and equal to the determined initial values.

$$T(x,0)=T_0 \;;\qquad T(y,0)=T_0 \qquad (3.14)$$

$$M(x,0)=M_0 \;;\qquad M(y,0)=M_0 \qquad (3.15)$$

Boundary conditions:

At the centre: For the symmetrical domain in the model, rate of temperature change and rate of moisture content change at the sample centre is equal to zero,

$$\frac{\partial T}{\partial x}=0 \quad ; \quad \frac{\partial M}{\partial x}=0 \; ; \; \frac{\partial T}{\partial r}=0 \quad ; \; \frac{\partial M}{\partial r}=0 \tag{3.16}$$

At the surface: At any time, energy transferred by convection from the oil to the product surface is equal to energy required for transferring heat to the centre of the product by conduction, for evaporating water from the product and for heating the water vapour evaporated from the product to oil temperature.

$$h\left(T_{sur}-T_{oil}\right)=-k\frac{\partial T}{\partial x}-\frac{k}{r}\frac{\partial (rT)}{\partial r}+\lambda\Gamma+\Gamma C_{pw}\left(T_{sur}-T_{oil}\right) \tag{3.17}$$

Rate of moisture diffusion by vapour flux within the product is equal to convective moisture transfer rate from the product surface to the oil.

$$h_m\rho\left(M_{sur}-M_{\omega}\right)=\frac{\partial(\rho DM)}{\partial x}+\frac{1}{r}\frac{\partial(r\rho DM)}{\partial r} \tag{3.19}$$

Where:

T = temperature (°C)

t = time (s)

x = axial distance in sample

y = radial distance in sample

r = radial distance in sample

k = thermal conductivity (W/m.K)

C_p = heat capacity of sample (J/kg.K)

C_{pw} = heat capacity of water (J/kg.K)

ρ = density (kg/m^3)

D = moisture diffusivity (m^2/s)

M = moisture content in (kg)

λ = heat of vaporization (J/kg)

h = heat transfer coefficient (W/m^2.K)

h_m = mass transfer coefficient (kg/m^2.s)

Subscripts *sur* and *oil* means surface and frying oil respectively.

The equations, initial conditions and boundary conditions were input into the simulation software and sweetpotato frying was simulated at typical frying conditions as discussed above.

4. RESULTS AND DISCUSSIONS

4.1 Density

Density was obtained in two different ways, multipycnometer and a mechanistic model.

4.1.1 Measured density

Density of sweetpotato was determined and modeled as a function of moisture content. Four moisture content levels of 0.75, 0.65, 0.55 and 0.45 were used. The result from the experiment is presented in Figure 4.1 and Table A1. Density was modeled as a function of moisture content (w.b) (equation 4.1). Coefficient of determination (R^2) was 0.97 and mean square error (MSE) was 156.1. For typical frying moisture content range, density was 1093-1203 kg/m^3.

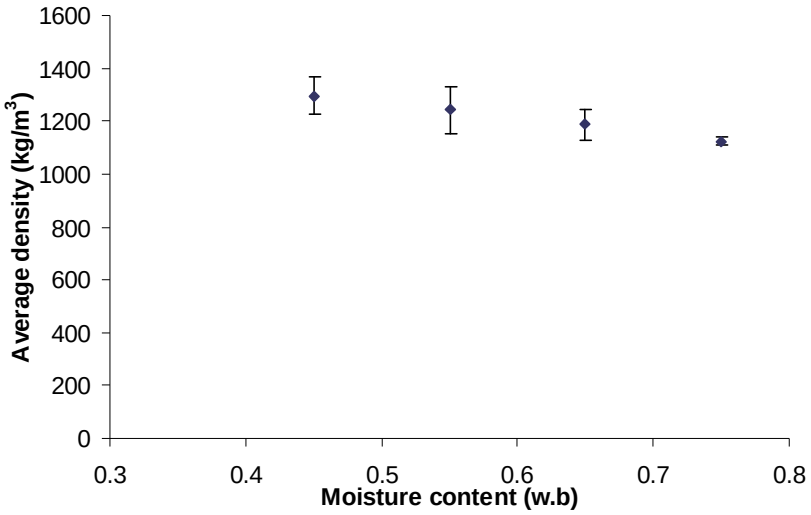

Figure 4.1: Average density of sweetpotato as a function of moisture content at 95% confidence level determined using a multipycnometer.

$$\rho = 1553 - 568.8m \qquad (4.1)$$

4.1.2 Density from mechanistic model

Density estimates from the mechanistic models yielded a result close to that of multipycnometer when average value for a moisture content level was compared. Mechanistic models developed for density of individual major components of food as a function of temperature, given in Table 3.1, was used to develop an empirical correlation predicting density of sweetpotato as a function of temperature and moisture content. The models in Table 3.1 give the contribution of each food component to density of sweetpotato at a particular temperature. Moisture content variation was simulated by varying the percentage of water in equation (3.3), which already includes the effect the

effect of temperature variation from the mechanistic models, using Excel. Density data was generated for temperature for temperature range of 20 to 180°C in steps of 10°C and moisture content range of 40 to 70% w.b. in steps of 1%. The regression model developed from the data generated using stepwise selection of variables (SAS Institute, Cary NC) is shown in equation (4.2). Direct comparison is impossible since density in multipycnometer was modeled as a function of moisture content only. A 3D mesh plot from SigmaPlot (Systat Software Inc, Richmond CA) of density as a function of temperature and moisture content is shown in Figure 4.2. Density of sweetpotato reduces with increase in both moisture content and temperature. This is attributed to the fact that an increase in temperature leads to higher moisture loss rate and shrinkage in sample leading to a lower volume. Although mass changes too, the rate of mass change (reduction) was lower than volume change. Predicted density range from the model for typical frying conditions (temperature and moisture content) was 1082-1193 kg/m^3. For sweetpotato at high moisture content, density is close to that of water.

$$\rho = 1491.5 - 0.573T - 496.8m \qquad (4.2)$$

Where:

ρ = density (kg/m^3)

T = temperature (°C)

m = moisture content (w.b.)

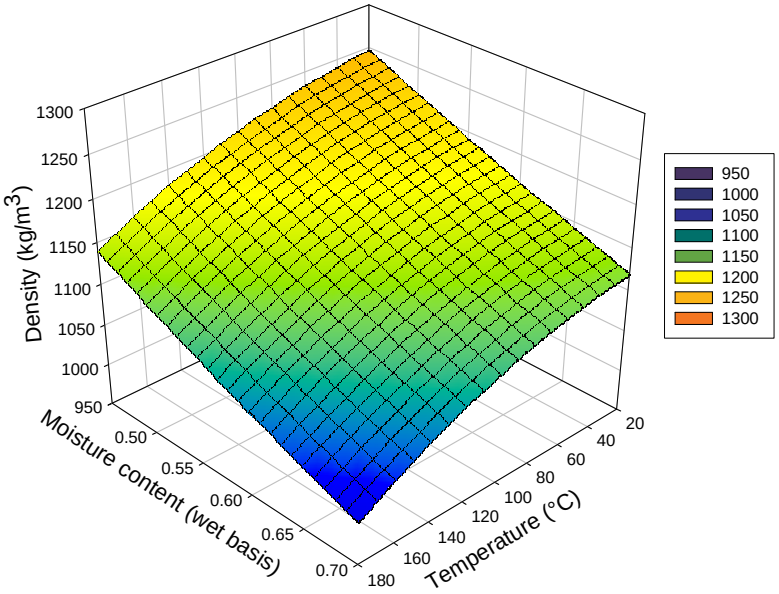

Figure 4.2: Density of sweetpotato as a function of moisture content and temperature determined from mechanistic model.

4.2 Specific heat capacity

Specific heat capacity, C_p of sweetpotato in this study was obtained by two methods namely differential scanning calorimeter (DSC) and mechanistic models of Choi and Okos (1985) as discussed in chapter 3. Results obtained from both methods are discussed below.

4.2.1 Specific heat from differential scanning calorimeter method

Specific heat was determined as a function of moisture content and temperature. Four levels of moisture content; 0.45, 0.55, 0.65 and 0.75 wet basis was used and scanning was done at 10°C/minute between 20 and 180°C. Experiment was conducted in duplicates. DSC is a comparison device. This

means that there is need to calibrate the device with a material of known specific heat value. The DSC was therefore first calibrated with water prior to the experiment on sweetpotato.

The result from the experiment is shown in Table A2. Figure 4.3 shows a 3D mesh plot of average C_p values from the experiment as a function of temperature and moisture content. It can be seen from the plot that C_p of sweet potato increases with both temperature and moisture content. Specific heat value obtained from the experiment ranged from 2250-3550 J/kg°C. The empirical correlation developed using stepwise selection of variables (SAS Institute, Cary NC) is shown in equation (4.3). R^2 was 0.97 and MSE was 3204.5. Predicted C_p range from the model for typical frying conditions (temperature range of 150 -180°C and moisture content range 0.45 -0.75(w.b)) was 3100-3250 J/kg°C.

$$C_p = 489.8 + 3313m + 24T - 53mT + 33.7m^2T \qquad (4.3)$$

Where:

C_p = specific heat (J/kg°C)

T = temperature (°C)

m = moisture content (w.b.)

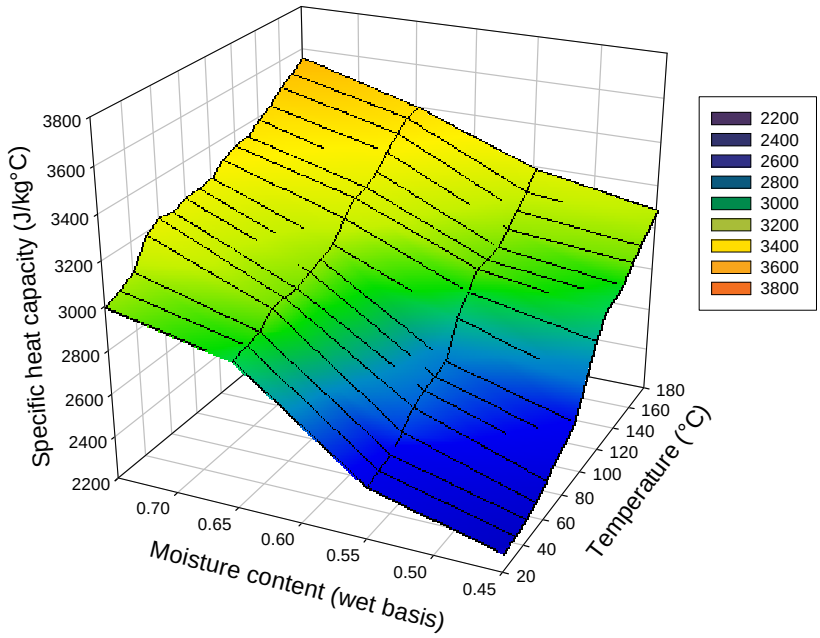

Figure 4.3: Specific heat capacity of sweetpotato as a function of temperature and moisture content (from DSC).

4.2.2 Specific heat from mechanistic model

Specific heat derived using developed models based on the work of Choi and Okos (1985) yielded a result close to that of DSC. Mechanistic models developed for specific heat of individual major components of food as a function of temperature, given in Table 3.1, was used to develop a model predicting specific heat of sweetpotato as a function of temperature and moisture content. The models in Table 3.1 give the contribution of each food component to specific heat of sweetpotato at a particular temperature. Moisture content variation was simulated by varying the percentage of water in equation (3.4),

which already included the effect of temperature variation from the mechanistic models, using Excel. Specific heat data was generated for temperature range of 20 to 180°C in steps of 10°C and moisture content range of 40 to 70% w.b. in steps of 1%. Specific heat increased linearly with increase in both temperature and moisture content.

A 3D mesh plot of average C_p value from the mechanistic model as a function of temperature and moisture content is shown in Figure 4.4. The regression model developed using stepwise selection of variables is shown in equation (4.4). Predicted C_p range from the model for typical frying conditions (temperature and moisture content) was 3145-3320 J/kg°C. Moreira and co-workers (1995) reported C_p of 2560 - 3360 J/kg.K for tortilla chip during frying. Rice and co-workers (1988) reported C_p of 2531 – 4015 J/kg.K for potato.

$$C_p = 1602.4 + 2543.2m + 0.92T - 9.8\times10^{-5}T^2 \qquad (4.4)$$

Where:

C_p = specific heat (J/kg°C)

T = temperature (°C)

m = moisture content (w.b.)

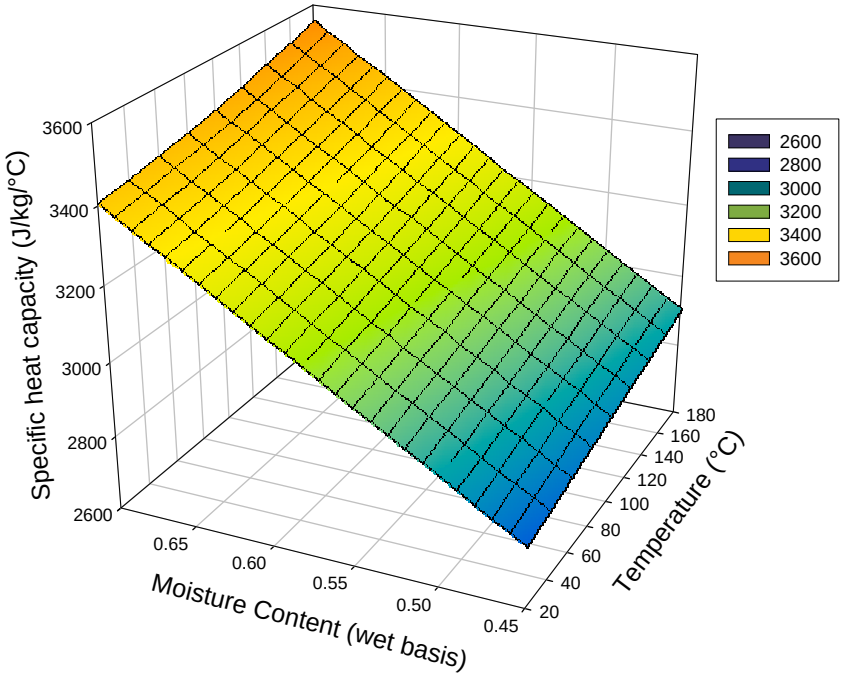

Figure 4.4: Specific heat capacity of sweetpotato as a function of temperature and moisture content (from mechanistic model).

4.3 Thermal conductivity

Thermal conductivity, *k* of sweetpotato determined from mechanistic model of Choi and Okos (1985) was a function of moisture content and temperature. Mechanistic models developed for thermal conductivity of individual major components of food as a function of temperature, given in Table 3.1, was used to develop a model predicting thermal conductivity of sweetpotato as a function of temperature and moisture content. The thermal conductivity models in Table 3.1 give the contribution of each food component by volume fraction to thermal conductivity of sweetpotato at a particular temperature. Moisture content variation was simulated by varying the percentage by volume

of water in equation (2.6), which already includes the effect the effect of temperature variation from the mechanistic models, using Excel. Thermal conductivity data was generated for temperature range of 20 to 180°C in steps of 10°C and moisture content range of 40 to 70% w.b. in steps of 1%. Thermal conductivity estimated with this method increased with increase in temperature and moisture content. Figure 4.5 shows a 3D mesh plot of thermal conductivity of sweet potato. The regression model developed is shown in equation (4.5). Predicted *k* range from the model for typical frying conditions (temperature and moisture content) is 0.43-0.54 W/m°C. The values are close to reported *k* values for similar product in literature. Buhri and Singh (1993) reported thermal conductivity of 0.552, 0.564 and 0.405 W/m°C for potato, carrot and green apple respectively at temperature range of 40-50°C.

$$k = 0.1613 + 0.0014T + 0.2924m + 3.4839 \times 10^{-7}T^2 \qquad (4.5)$$

Where:

k = Thermal conductivity (W/m°C)

T = temperature (°C)

m = moisture content (w.b.)

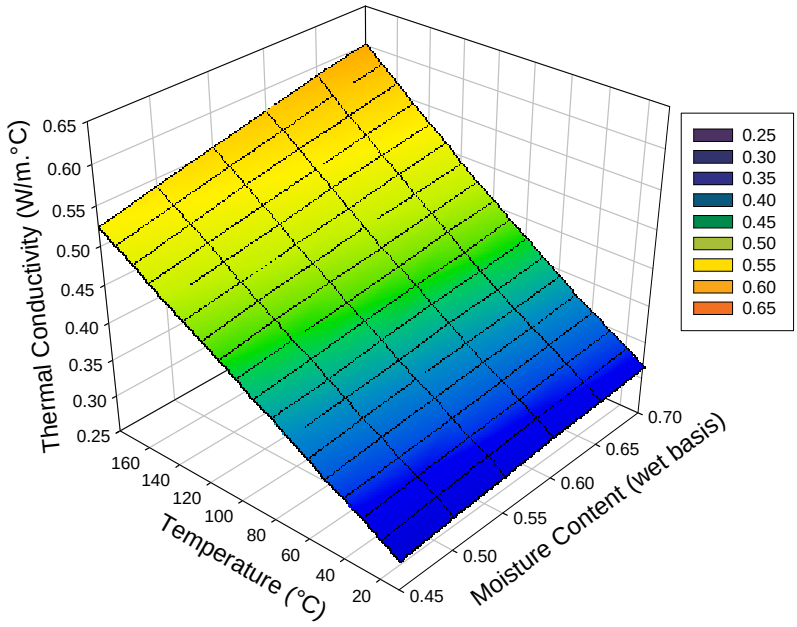

Figure 4.5: Thermal conductivity of sweetpotato as a function of moisture content and temperature (from mechanistic model).

4.4 Thermal diffusivity

Thermal diffusivity, α of sweet potato was determined as a function of moisture content and temperature from mechanistic model of major food components. Mechanistic models developed for thermal diffusivity of individual major components of food as a function of temperature, given in Table 3.1, was used to develop a model predicting thermal diffusivity of sweetpotato as a function of temperature and moisture content. The thermal diffusivity models in Table 3.1 give the contribution of each food component to thermal diffusivity of sweetpotato at a particular temperature. Moisture content variation was simulated by varying the percentage by volume of water in equation (3.7), which

already included the effect the effect of temperature variation from the mechanistic models, using Excel.

Thermal diffusivity data was generated for temperature range of 20 to 180°C in steps of 10°C and moisture content range of 40 to 70% w.b. in steps of 1%. Thermal diffusivity of sweetpotato determined by this method generally increased with increase in moisture content and temperature. Figure 4.6 shows a 3D mesh plot of thermal diffusivity of sweet potato. The regression model developed using stepwise selection of variables of SAS is shown in equation (4.6). Predicted α range from the model for typical frying conditions (temperature and moisture content) is 1×10^{-7} -1.3×10^{-7} m^2/s. This was comparable with 1.1×10^{-7} m^2s^{-1} reported for sweetpotato by Wadsworth and Spadaro (1969). Matthews and Hall (1968) reported α value of 1.33×10^{-7} m^2/s and 1.37×10^{-7} m^2/s for raw and cooked potato respectively.

$$\alpha = 7.32\times10^{-8} + 3.41\times10^{-10}T + 2.1\times10^{-8}m + 5.31\times10^{-13}T^2 \qquad (4.6)$$

Where:

α = thermal diffusivity (m^2/s)

T = temperature (°C)

m = moisture content (w.b.)

An estimate of α was also made from thermal conductivity, specific heat and density from equation (2.10) for comparison. The value compared well with predicted vales from equation (4.6) above.

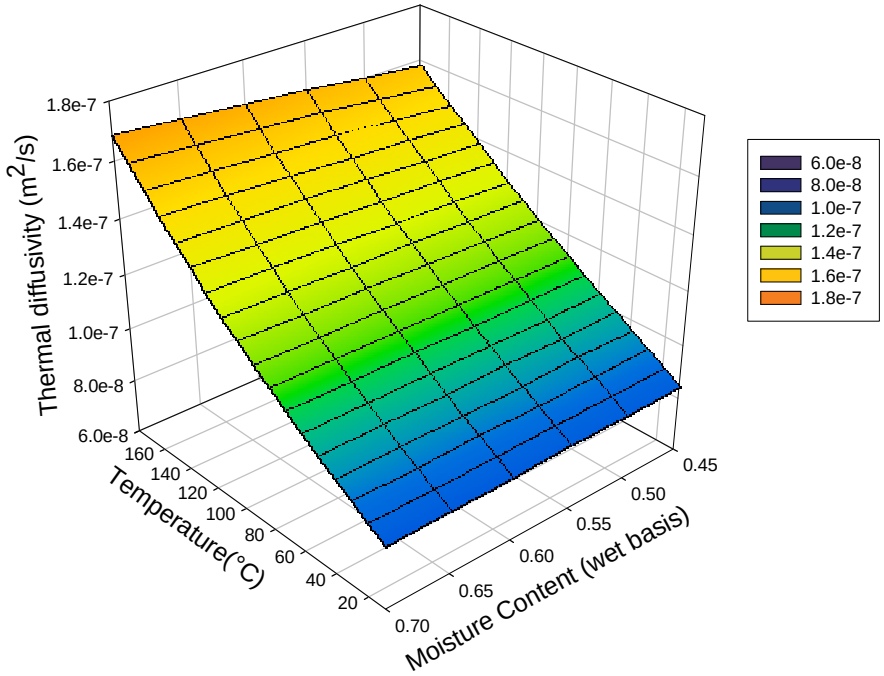

Figure 4.6: Thermal diffusivity of sweetpotato as a function of moisture content and temperature (from mechanistic model).

4.5 Moisture content during frying

Moisture content during frying was measured at specific periods of 0, 30, 60, 120, 180, 240 and 300 s of frying. Separate experiments were run for whole sample, crust part and the core part of the product. Three sample sizes and four oil temperature were used in frying and the experiment was conducted in duplicate. Table A3 and A4 show the result from the experiment. All results are in decimal (wet basis). Initial moisture content in sweet potato were as high as 0.82. As expected, moisture content reduced during frying. The moisture loss rate was quite high at the beginning of frying as moisture on the surface of the sample evaporated. The moisture loss rate however reduced as frying

progressed. It was observed that rate of moisture loss was higher for a smaller sample size and also higher for higher oil temperature (Figure 4.7 and 4.8). This same trend was observed for the three groups of moisture content (whole, crust, core) determined.

The rate of moisture loss during frying has been expressed as the ratio of a driving force to resistance from the product (Rice and Gamble, 1989). The driving force is provided by the conversion of water to steam by heat. As frying temperature increased, the moisture content for the same frying time decreased since an increase in temperature resulted in a higher kinetic energy for water molecules leading to a more rapid moisture loss in form of vapour which ultimately reduced the moisture content of the product (Farinu and Baik, 2005). Also, heat conduction to the center of food is faster for a product with smaller dimension (diameter to thickness ratio in this case) leading to water molecules at the center of this smaller product having a higher kinetic energy at any particular time during frying and therefore, experience higher moisture loss rate than a bigger sample. Krokida and co-workers (2000) also demonstrated that oil temperature has a negative effect on the moisture content of French fried potatoes.

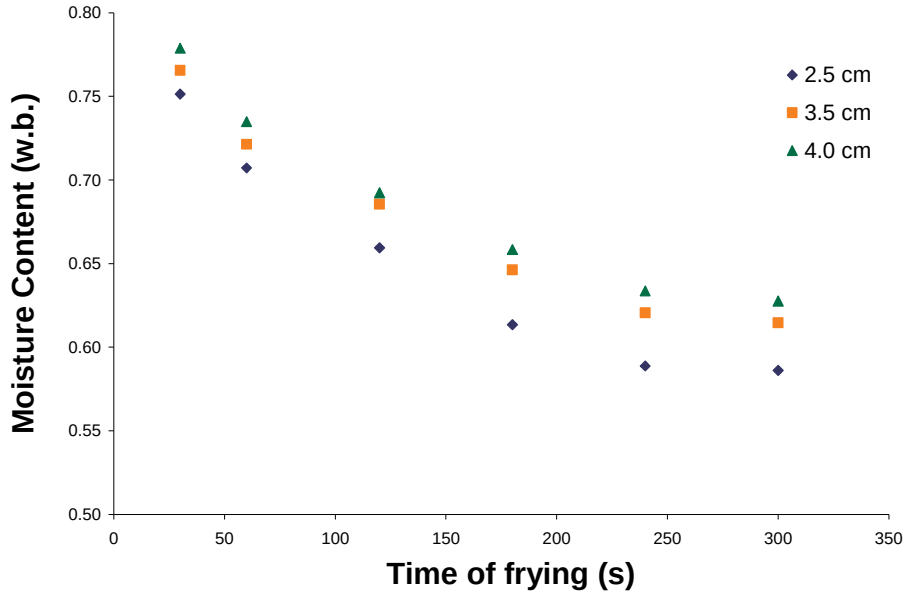

Figure 4.7: Moisture content variation among sizes for sample (whole sample) fried at 180°C.

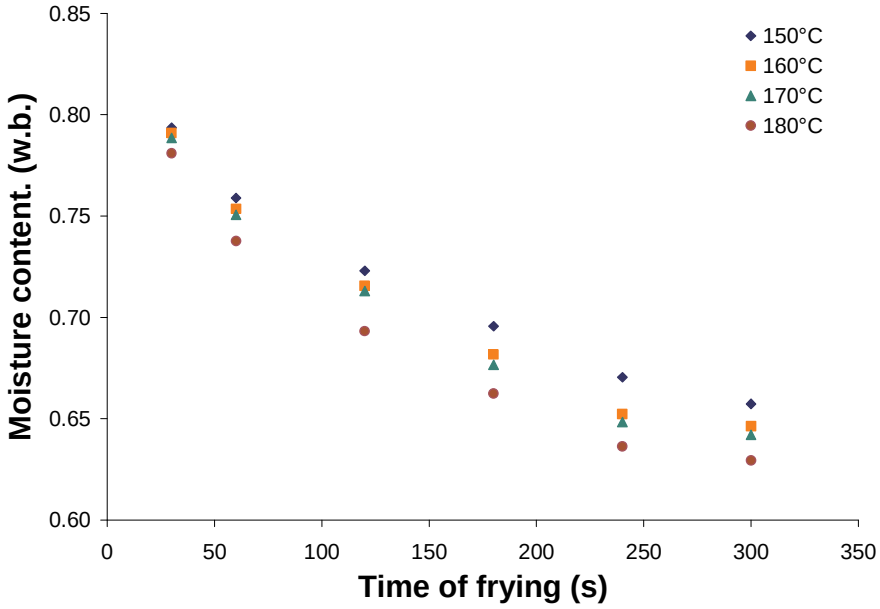

Figure 4.8: Moisture content of big sample (D/L=4) during frying at four different oil temperatures.

4.6 Temperature during frying

Temperature was measured at 5 different locations in the sample. Table A5 and A6 show a summary of temperature measured during frying. Temperature at the surfaces of the sample rose rapidly at the beginning of frying and typically reached a stable value (usually about 6 to 9°C below the oil temperature) after about 45 s of frying. The bottom surface temperature was usually higher than the top surface temperature at the beginning of frying. The top surface temperature however caught up with bottom counterpart after about 50 s of frying. This trend is believed to be due to the fact that the bottom surface receives more direct heat than the top at the beginning of frying before significant bubbling started. However, the occurrence of vapour bubbling close to the surface of the sweetpotato after the initial period increased the heat transfer coefficient and therefore the temperature at the top surface.

The trend of temperature profile at the center and the two intermediate locations of the sample were quite similar. The temperature rose with progress in frying until it reached the boiling point of water, 100°C. The temperature then remained stable for some time since the heat supplied was being spent on moisture evaporation at this stage. After some time, the temperature started to increase again. Figure 4.9 and 4.10 shows the typical temperature curves during frying. It is noteworthy to mention that the temperature of the intermediate locations (between the surfaces and the center) remained at 100°C until the sample center temperature has reached boiling point (100°C) and stayed there for some time. This is understandable since the bulk of moisture lost from the center will pass through these locations before it gets to the surface and is lost

in the oil as vapour. Temperature within the product was found to increase with oil temperature no matter what two sizes are being compared. Average product temperature during frying was also found to vary inversely with sample size. The smallest sample had highest temperature for a particular time during frying and *vice versa*. This is due to a smaller thermal gradient across the smaller sample profile which means that heat is conducted faster within the product.

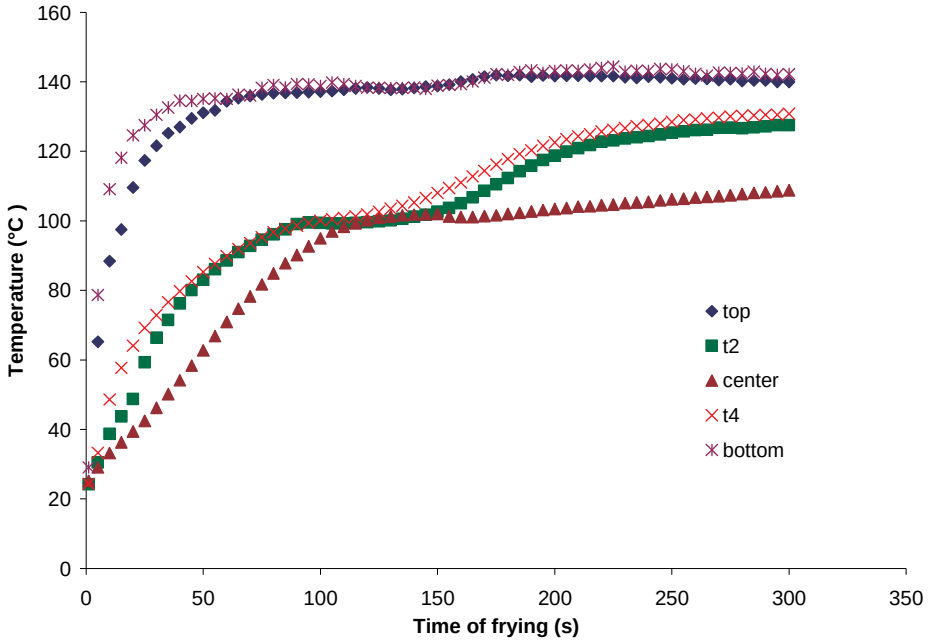

Figure 4.9: Temperature of medium sample (D/L=3.5) during frying at 150°C (D= sample diameter, L= sample thickness). t2 and t4 are temperature of positions along the sample thickness in between top and center, and bottom and center respectively.

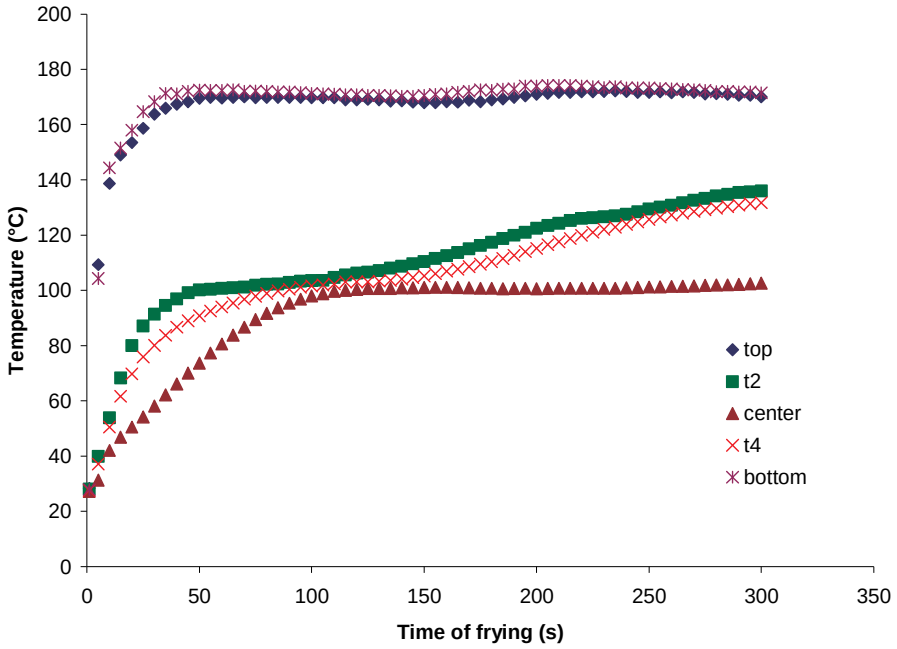

Figure 4.10: Temperature of medium sample (D/L=3.5) during frying at 180°C. (D= sample diameter, L= sample thickness). t2 and t4 are temperature of positions along the sample thickness in between top and center, and bottom and center respectively.

4.7 Heat transfer coefficient

Average heat transfer coefficient, *h* was determined for each of the six time periods (0-30, 30-60, 60-120, 120-180, 180-240 and 240-300 s) during frying based on heat energy balance. Resulting *h* values are shown in Table A7 and A8. Heat transfer coefficient rose quickly at the beginning of frying and peaked at about 50-80 seconds of frying depending on the oil temperature of frying. There is significant bubbling due to rapid moisture loss at the early stage of frying. The rate of increase of *h* is higher for a higher oil temperature. This is

due to the lower viscosity of oil at higher temperature and higher drying rate and bubbling/oil agitation which further increases the heat transfer coefficient. The maximum *h* reached during frying is higher for higher oil temperature (Figure 4.11). After reaching the maximum, h during frying decreases and stabilizes at 450-550 W/m^2°C for the remaining period of frying.

Heat transfer coefficient at the latter period of frying is slightly higher for frying done at lower oil temperature. This is probably due to some slightly significant bubbling in this period for frying done at lower oil temperature since the initial drying rate is lower. Generally, *h* is higher for smaller sample than for bigger sample fried at the same temperature (Figure 4.12). This is due to higher product volume temperature in smaller samples since dimension is smaller and heat transfer rate to product center is faster.

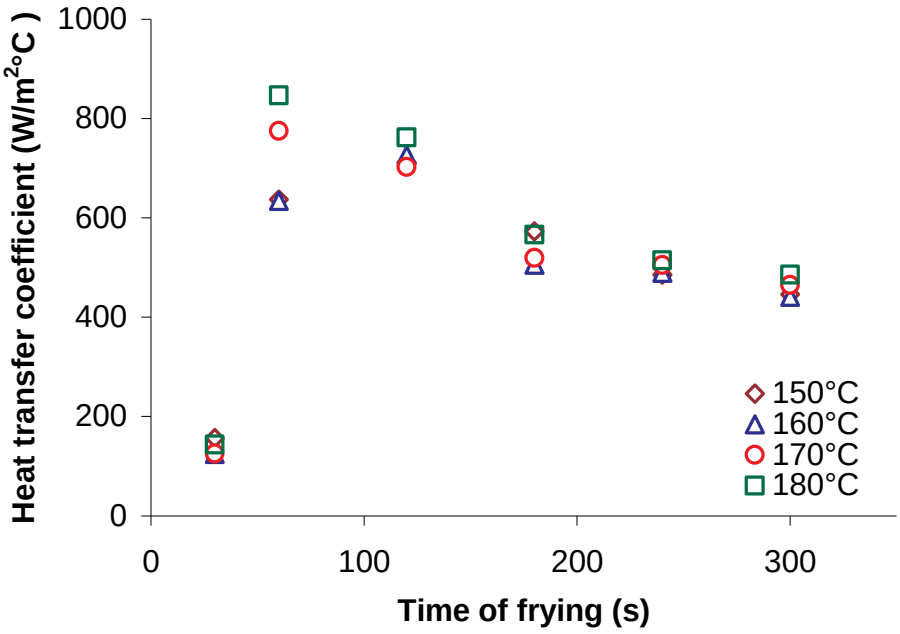

Figure 4.11: Heat transfer coefficient determined for medium sample (D/L=3.5).

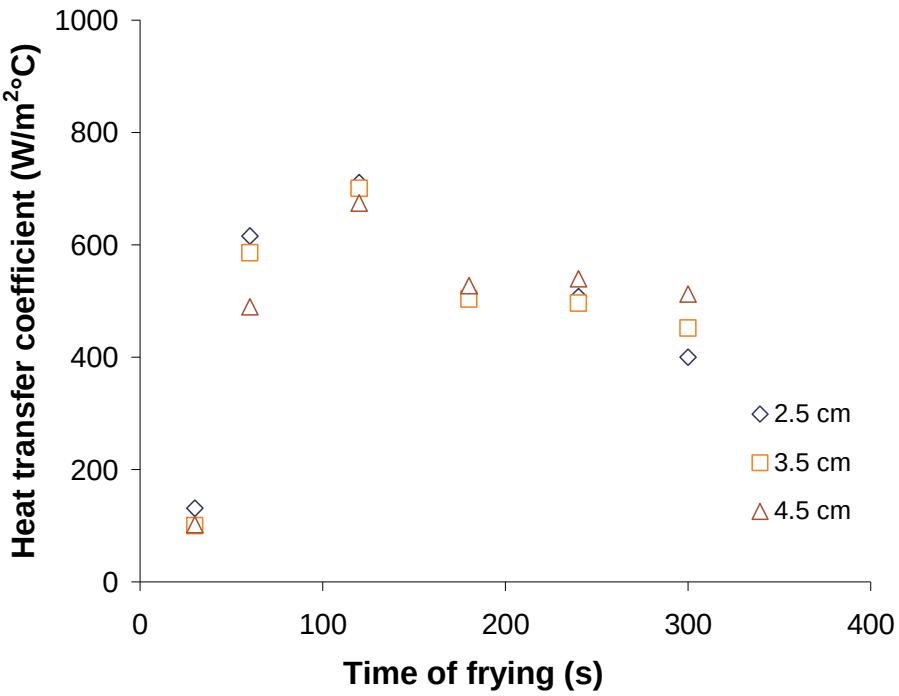

Figure 4.12: Heat transfer coefficient determined for samples fried at 150°C.

4.8 Computer simulation of sweetpotato during frying

Heat transfer and moisture transfer during frying of sweetpotato was simulated using the heat transfer and diffusion modules of COMSOL multiphysics. Governing equations, boundary conditions and initial conditions are as defined in chapter 3. Computer modeling was done through the graphical user interphase and the MATLAB prompt of the software. The built-in equation for diffusion in the software was given in equation (3.13) and was found to suffice for the purpose of this study. However the heat transfer equation (equation 3.11) and its associated boundary conditions were user-defined.

Figures 4.13 and 4.14 show typical domain plots for temperature and moisture content respectively after 300 s of frying simulation.

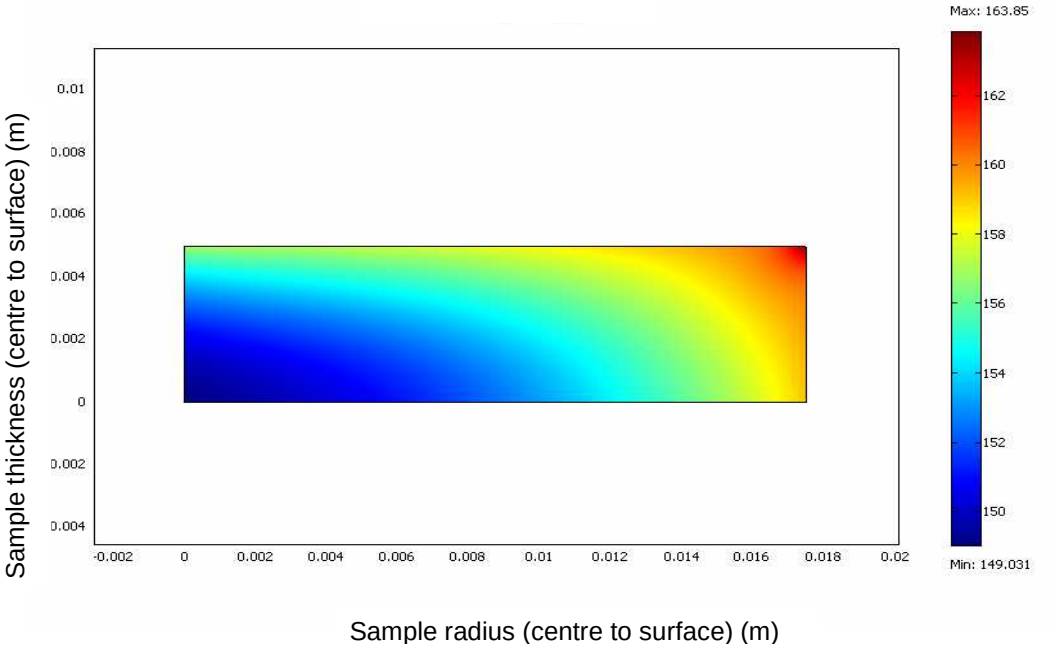

Figure 4.13: Simulated temperature profile of medium sample (D/L=3.5) fried at 170°C for 300 s.

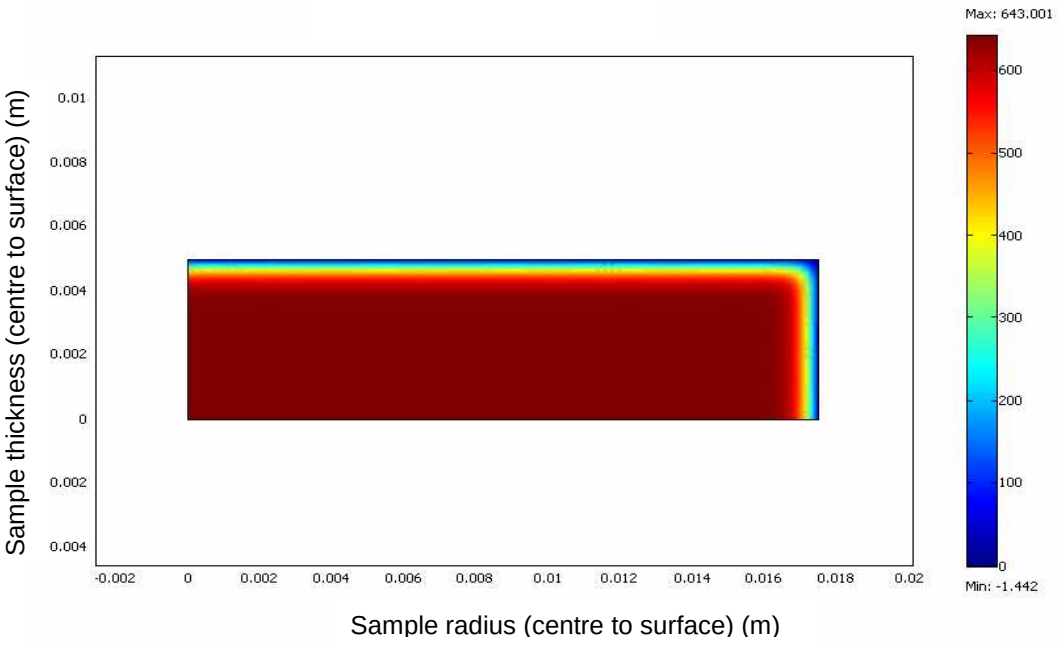

Figure 4.14: Simulated moisture content profile of medium sample (D/L=3.5) fried at 170°C for 300 s.

4.8.1 Comparison between temperature profiles of experiment and simulation

Two separate temperature profiles (sample surface and sample centre) were used to fit simulation to the experiment. A perfect fit was obtained for the surface temperature for all the cases. The centre temperature however did not record the same total success. Centre temperature profile from the simulation matched perfectly, in most cases, with that of the corresponding experiment until it reached 100°C then there was deviation. While centre temperature from the experiment climbed to 100°C and stabilized at 100°C for some time (60 -100 s) before it started to rise again, centre temperature from the simulation observed a shorter period of temperature stability before it started rising again. Some of the reasons thought to be responsible for this difference are:

1. The assumption that thermophysical properties of the crust and core regions are same during frying is not strictly true. The crust is a dry porous matrix that serves as an insulating material during frying and its thermophysical properties varied from that of the core. This affected the simulation result. Simulating each section with different but correct thermal properties would yield a better result.
2. During frying, there is condensation on the thermal probes inserted into the sample as they have been at a lower temperature than the sample being measured. The condensate insulated the probes and the temperature measured might have been slightly understated.

Attempts were however made to strike the best balance possible in fitting

both data. Figures (4.15 and 4.16) shows comparison between experimental and simulation temperature profiles for sample size 3.5 cm fried at 160°C. Average deviation between experiment and simulation for surface temperature is 2.49°C while average deviation for centre temperature is 9.5°C.

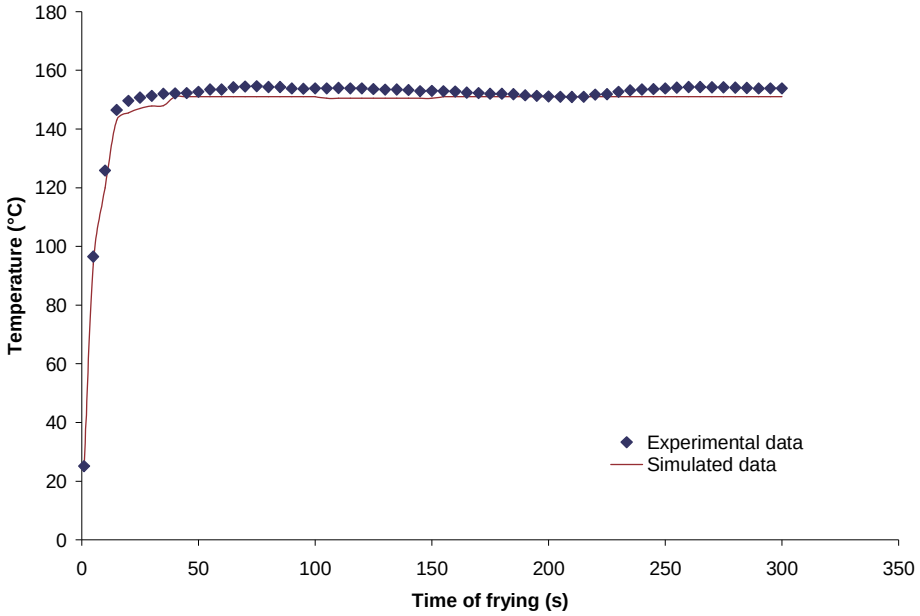

Figure 4.15: Comparison of sample's surface temperature of experiment and simulation for medium sample (D/L=3.5) fried at 160°C

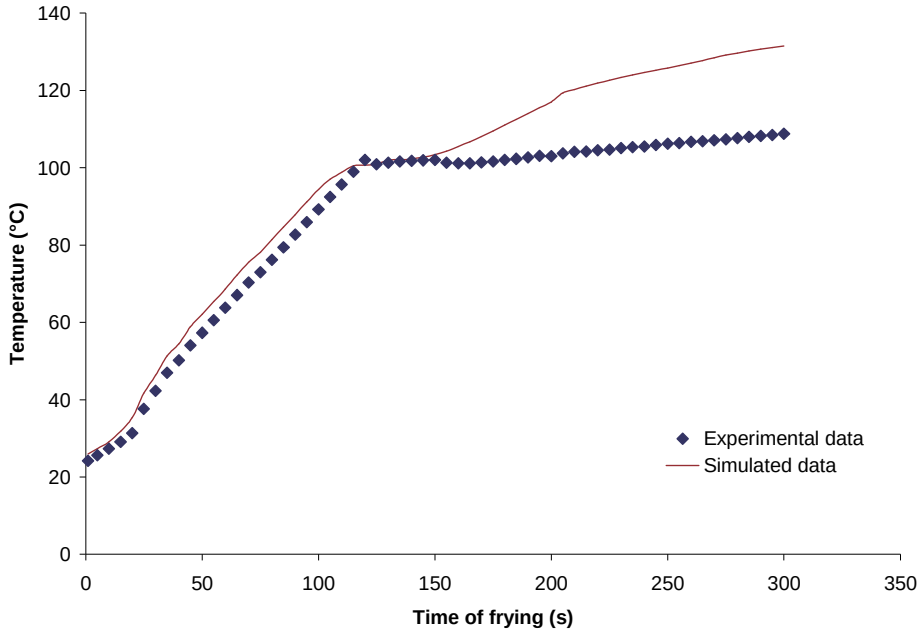

Figure 4.16: Comparison of sample's centre temperature of experiment and simulation for medium sample (D/L=3.5) fried at 160°C

4.8.2 Comparison between experimental and simulated moisture content

Two separate moisture content profiles (sample surface - crust and whole sample) were used to fit simulation to the experiment. Similar to the case of temperature, a perfect fit was obtained for the crust moisture content for all the cases. The whole sample moisture content's fit however was not as perfect as that of crust. Slight difference was observed at the early stage of frying between experimental and simulation moisture content data, and this difference only increased with frying time. Some of the reasons thought to be responsible for this difference are:

1. Frying is a moving boundary problem in which a water evaporation front is established on the product surface at the beginning of frying as water

leaves the sample and this front gradually approaches the sample centre as frying progresses leaving behind a porous matrix called crust. This means that there was evaporation taking place inside the sample as frying progressed. Moisture vapour flux was assumed to diffuse from the sample into the oil at the sample surface. Coupling vapour flux at the sample surface as was done in this study might therefore not represent the process perfectly as it does not totally cater for this gap in moisture loss inside the sample as frying progresses. Introducing this factor into the surface boundary condition would lead to a better result.

2. The difference in thermophysical properties of crust and core regions also would affect the moisture loss rate. Determining the actual properties of the crust region and simulating the process with these values would lead to a better result.

Simulation was done in such a way as to make provision for these issues and to obtain the best fitting possible from practical point of view. Figures (4.17 and 4.18) shows comparison between experimental and simulation moisture content profiles for 3.5 cm sample fried at 150°C. Average deviation between experiment and simulation for surface moisture content was 7.26 kg/m^3 while average deviation for whole sample was 28.34 kg/m^3.

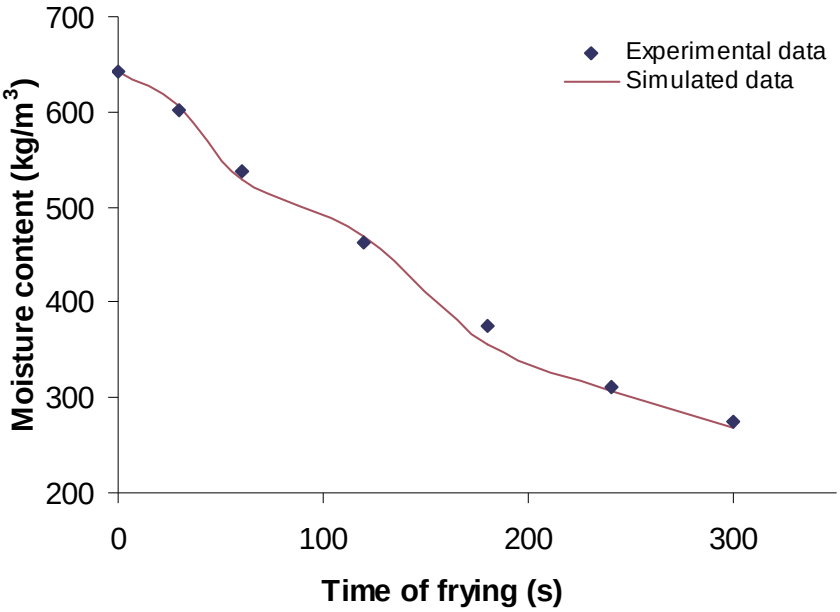

Figure 4.17: Comparison of surface moisture content profiles of experiment and simulation of medium sample (D/L=3.5) fried at 150°C.

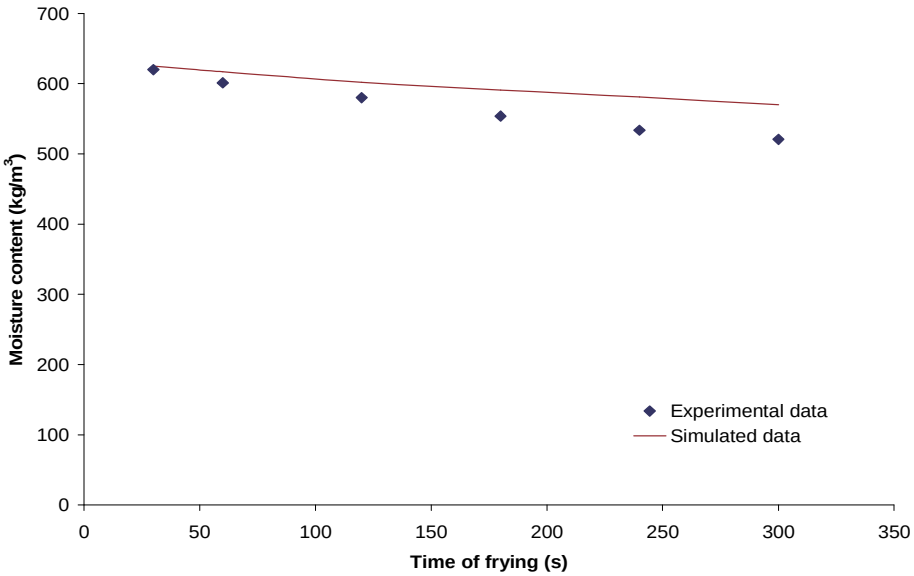

Figure 4.18: Comparison of core moisture content profiles of experiment and simulation of medium sample (D/L=3.5) fried at 150°C

4.8.3 Mass transfer coefficient

Mass transfer coefficient values from the simulation are presented in Table A9 and A10. The trend observed in the result is that h_m increased at the onset of frying as the sample gained heat and water from sample evaporates starting with the surface moisture. The coefficient increased with time of frying as the moisture loss rate increases. However towards the end of frying, h_m decreased as the moisture loss rate decreased. This is explained by the decrease in moisture content of the sample at the latter stage of frying hence a reduction in the vapour bubbling and oil agitation which had before that period been driving the heat transfer coefficient and moisture loss rate. A typical h_m profile during frying is shown in Figure 4.19.

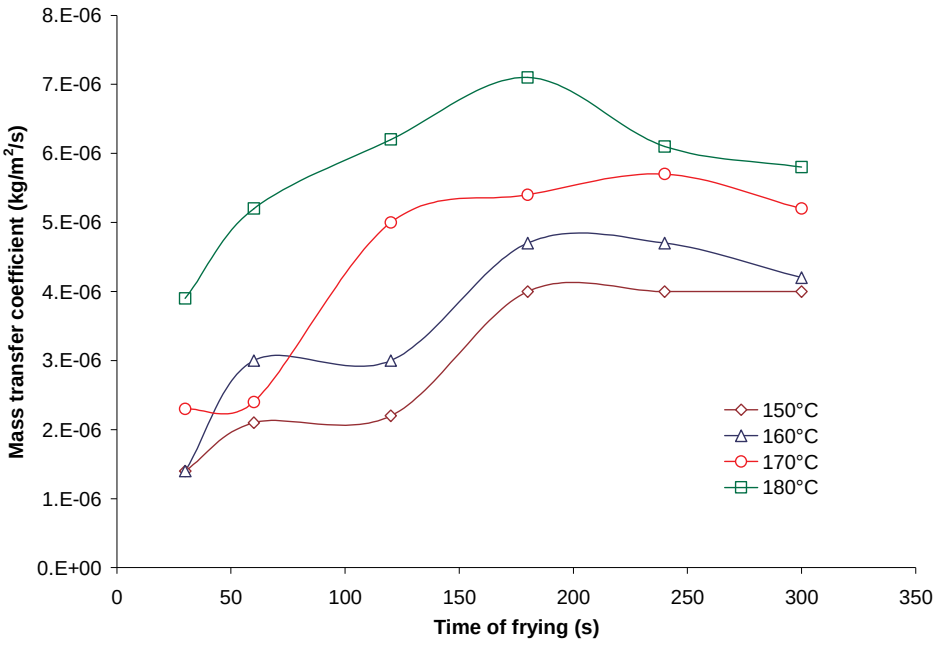

Figure 4.19: Mass transfer coefficient determined during simulation of medium sample (D/L=3.5) frying.

4.9 Correlation between heat transfer coefficient, *h* and mass transfer coefficient, h_m

An attempt was made at developing a relationship between heat transfer coefficient, *h* and mass transfer coefficient, h_m. The trend observed for both parameters were different. While *h* rose sharply at the commencement of frying reaching a maximum before 100 s of frying and settling to an almost stable value for the last 120 s of frying in most cases (Figure 4.11), h_m rose gradually and continued rising for the most part of frying and did not reach a maximum until around 200 s of frying in most cases (Figure 4.19).

Heat transfer coefficient and mass transfer coefficient reached maximum values at separate times during frying. Heat transfer coefficient, *h* and mass transfer coefficient, h_m data were analysed for possible relationship. No direct relationship was found between them. Both parameters were found to be a function of experimental factors (sample size, oil temperature and frying time) at different levels and cannot be directly correlated in a general form. However, a relationship was found to exist between maximum *h* and the corresponding h_m at that point. The relationship found between them is shown in equation (4.7) with R^2 of 0.91 and p value of <0.001. Summarised ANOVA table for the model is shown in Table B1.

$$h_{m1} = -9\times10^{-11} h_{\max}{}^2 + 2\times10^{-7} h_{\max} - 6\times10^{-5} \qquad (4.7)$$

Maximum *h* and maximum h_m during frying were also correlated and the relationship found to exist between them is shown in equation (4.8) with R^2 of 0.83 and p value of <0.001. Summarised ANOVA table for the model is shown in Table B2.

$$h_{m2} = -8\times10^{-11} h_{\max}{}^{2} + 1\times10^{-7} h_{\max} - 5\times10^{-5} \quad (4.8)$$

Where:

h_{max} = maximum heat transfer coefficient reached during frying (W/m^2.°C)

h_{m1} = mass transfer coefficient at maximum heat transfer coefficient (kg/m^2.s)

h_{m2} = maximum mass transfer coefficient reached during frying (kg/m^2.s)

Equations (4.7) can be used to determine the corresponding mass transfer coefficient during sweetpotato frying from the value of the maximum heat transfer coefficient. Equation (4.8) can be used to determine the maximum mass transfer coefficient from the value of the maximum heat transfer coefficient during sweetpotato frying. These equations can also be used to estimate a rough approximation during deep fat frying of similar food product like potato.

4.10 Effects of experimental factors on *h* and h_m

The effects of experimental factors (oil temperature, sample size and time of frying) were investigated and SAS stepwise regression was used to select significant variables in developing a regression model for *h* and h_m as a function of these factors. The models developed for *h* and h_m are as shown in equations (4.9) and (4.10) with R^2 of 0.90 and 0.76 respectively. The p-values were <0.001 and 0.012 respectively. Summarised ANOVA tables for the models are shown in Table B3 and B4.

$$h = 1.28T_{oil} - 1.5\Delta T^{2} + 0.36T_{oil}\Delta T - 1.2dT_{oil} - 10.5 \quad (4.9)$$

$$h_m = 9.3\times10^{-8}T_{oil} - 8.6\times10^{-7}d - 1.9\times10^{-7}\Delta T + 2.1\times10^{-6}\Delta T^{2} - 6\times10^{-6}. \quad (4.10)$$

Where:

h = heat transfer coefficient (W/m^2°C)

h_m = mass transfer coefficient (kg/m^2.s)

T_{oil} = oil temperature (°C)

d = sample diameter to thickness ratio *i.e.* D/L

$\Delta T = T_{oil} - T_{surface}$ (°C), ΔT is a physical parameter representing progression of frying.

From experimental observations and developed models, h and h_m were found to have direct positive relationships with oil temperature and an inverse relationship with sample size. Equations (4.9) and (4.10) can be used to predict the heat transfer and mass transfer coefficients during deep fat frying of sweetpotato or rough estimate of h and h_m of products with similar properties if the product temperature and moisture content are known. The applicability of these equations will be within the moisture content and temperature range used in developing them, 0.45-0.75 w.b. and 20-180°C respectively.

5. SUMMARY, CONCLUSIONS AND RECOMMENDATIONS

5.1 Summary and conclusions

The general objective of this thesis research was to study the relationship between heat and mass transfer coefficients during deep fat frying of sweetpotato. In doing this, the thermophysical properties of the crop had to be determined. Thermal conductivity, *k* of sweetpotato increased during frying. As frying progressed, the product lost moisture but temperature also increased. The net effect is a rise in *k* from an average of 0.43 W/m°C at the inception of frying to 0.54 W/m°C after about 30 s of frying and 0.5 W/m°C towards the end of frying. This same low-high-low trend was observed for thermal diffusivity with a range of 1×10^{-7} to 1.3×10^{-7} m^2/s and specific heat with a range of 3145 - 3320 J/kg°C during frying.

Density determined from the conducted experiment was modeled as a function of moisture content only. The range of sweetpotato density during frying was 1093 to 1203 kg/m^3. For sweetpotato sample before frying (moisture content of 0.81 - 0.82 wet basis), density was close to that of water. During frying, temperature at the surface of the sample rose sharply reaching a stable value (6 - 9°C below oil temperature) within 30 s. Temperature inside the sample rose gradually, usually stable for some time at 100°C as moisture evaporated

before further increase. Moisture loss rate was also rapid for the sample surface than the core.

Heat transfer coefficient, *h* was estimated based on energy balance during frying and was found to approach a maximum between 80 and 140 s of frying depending on the oil temperature and sample size. The range of maximum *h* reached was 700 - 850 W/m^2°C. Maximum *h* reached varied directly with oil temperature but inversely with sample size. *h* at latter period of frying (200 - 300 s) was 450 - 550 W/m^2°C. Mass transfer coefficient, h_m determined from finite element computer simulation was found to reach a maximum (4×10^{-6} to 7.2×10^{-6} kg/m^2.s) after 200 s of frying in most cases. Both *h* and h_m were found to increase with increase in oil temperature but decrease with increase in sample size. No general correlation exists between *h* and h_m. However, a positive quadratic correlation existed between maximum *h* and maximum h_m during frying. Maximum *h* also varies directly with the corresponding h_m at that point. All models and empirical correlations developed in this study as a function of temperature and moisture content are valid for typical frying condition range (Temperature: 20 - 180°C and Moisture content: 0.45 - 0.75 (w.b.))

5.2 Recommendations

The relationship between heat transfer coefficient, *h* and mass transfer coefficient, h_m during deep fat frying of sweetpotato was investigated in this study. It is expected that the study would provide an insight into the general pattern of correlation between *h* and h_m during frying and most other drying processes. Specific situation for other processes and food products, however,

had to be studied since processes differ and thermophysical properties vary from food to food. Frying is a moving-boundary problem in which a previously non-existent moisture evaporation front is established on the food surface and it moves towards the centre during frying. This phenomenon accounts for the crust and the core parts of the sample which were not separated in this study. Their properties actually vary slightly and this can be studied and incorporated into the simulation in a future study. This could be achieved by incorporating separate governing equations for heat and mass transfer for the crust and core regions which will take into consideration the difference in their thermophysical properties.

There are usually structural changes during deep fat frying. This is in form of puffing after about 30 seconds of frying and shrinkage of sample towards the end of frying. The simulation work in this study did not account for structural change beyond the change in density during frying. It is recommended that a future study incorporates this effect. Finally, for optimization of the frying process, more work is required on energy consumption model and kinetics of quality changes in the product (color, texture, nutritional index, *etc.*) and the results should be coupled with the transport phenomena model.

REFERENCES

AOAC. 2002. AOAC official method 984.25. In *Official Methods of Analysis of AOAC International*, 17th ed., Vol. 2, Gaithersburg, MD: The Association of Official Analytical Chemists International.

Arce, J.A., V.E. Sweat and K. Wallapapan. 1980. Thermal diffusivity and conductivity of soy flour. ASAE Paper No. 6528. St. Joseph, MI. American Society of Agricultural Engineers.

Ateba, P. and G.S. Mittal. 1994. Modelling the deep fat frying of beef meatballs. *International Journal of Food Science and Technology.* 29: 429-440.

Baik, O.D. (2004). Finite Element Method. In *ABE898: Modelling of Food Process Lecture Notes*. University of Saskatchewan.

Baik, O. D. and G.S. Mittal. 2002. Heat transfer coefficients during deep-fat frying of tofu disc. *Transactions of the American Society of Agricultural Engineers.* 45: 1493-1499.

Bengtsson, N.E. and B Jakobsson 1974. Microwave Energy Applications Newsletter 6(3).

Brailsford, A.D. and K.G. Major. 1964. Thermal conductivities of aggregates of several phases, including porous materials. *British Journal of Applied Physics*. 15: 313-319.

Brodkey, R.S. and H.C. Hershey. 1988. *Transport Phenomena: A Unified Approach*, Nueva York: McGraw-Hill. 516-520.

Buhri, A.B. and R.P. Singh 1993. Measurement of food thermal conductivity using differential scanning calorimetry. *Journal Food Science*. 58: 1145.

Califano, A.N. and A. Calvelo. 1991. Thermal conductivity of potato between 50 and 100°C. *Journal of Food Science.* 56(2):586-587

Charney, P. and R.A. Seelig. 1967. *Fruit & Vegetable Facts & Pointers: Sweetpotatoes.* Washington, D.C.: United Fresh Fruit & Vegetable Association,

Chen, H., B.P. Marks and R.Y. Murphy. 1999. Modeling coupled heat and mass transfer for convection cooking of chicken patties. *Journal of Food Engineering*. 42: 139-146.

Choi, Y. and M. R. Okos. 1983. The thermal properties of tomato juice concentrates. *Transactions of the ASAE,* 26(1): 305-311.

Choi, Y and M.R. Okos. 1985. Effects of temperature and composition on the thermal properties of foods. In *Food Engineering and Process Applications*. Vol. 1. ed. M. Lemaguer and P. Jelen, 93. London, UK: Elsevier.

COMSOL™. 2005. COMSOL™ Multiphysics: Model Library - Heat Transfer Module. Los Angeles. 192-202.

Costa, R.M., F.A.R. Oliveira, O. Delaney and V. Gekas. 1999. Analysis of the heat transfer coefficient during potato frying. *Journal of Food Engineering,* 39(3): 293-299.

Derdour, L. and H. Desmorieux. 2004. A model for internal moisture diffusivity during the regular regime: Comparison with experimental data obtained on plaster and spirulina*. Proceedings of the 14th International Drying Symposium. São Paulo, Brazil,* 22-25 August, A: 718-725.

Drouzas, A.E., Z.B. Maroulis, V.T. Karathanos and G.D. Saravacos. 1991. Direct and indirect determination of the effective thermal diffusivity of granular starch. *Journal of Food Engineering*, 13(2): 91-101.

Farkas, B.E. and L.J. Hubbard. 2000. Analysis of heat transfer during immersion frying. *Drying Technology*, 18(6): 1269-1285.

Farkas, B.E., R.P. Singh and T.R. Rumsey. 1994. Modeling the effect of properties and process conditions in food frying. *Annual meeting of Institute of Food Technologist.* Atlanta, GA.: Institute of Food Technologists.

Farkas, B.E., R.P. Singh and T.R Rumsey. 1996a. Modeling heat and mass transfer in immersion frying: model development*. Journal of Food Engineering,* 29: 211–226.

Farkas, B.E., R.P. Singh and T.R. Rumsey. 1996b. Modeling heat and mass transfer in immersion frying: model solution and verification. *Journal of Food Engineering,* 29: 227–248.

Farinu, A. and O. –D. Baik. 2005. Deep fat frying of foods: Transport phenomena. *Food Reviews International*. 21: 389-410.

Farral, A.W., A.C. Chen, P.Y. Wang, A.M. Phanak, T. Hendrick and D.R. Heldman. 1970. Thermal conductivity of dried milk in a packed bed. *Transactions of ASAE,* 13(3): 391-394.

Gamble, M.H. and P. Rice. 1987. Effect of pre-frying drying on oil uptake and distribution in potato crisp manufacture. *International Journal of Food Science and Technology,* 22: 535–548.

Gamble, M.H. and P. Rice. 1988. Effect of initial tuber solid content on final oil content of potato chips. *Lebensmittel Wissenschaft und Technologie*, 22: 62-65.

Gupta, T.R. 1990. Specific heat of Indian unleavened flat bread (chaphati) at various stages of cooking. *Journal of Food Process Engineering*, 13(2): 217-227.

Hubbard, L.J. and B.E. Farkas. 1999. A method of determining the convective heat transfer coefficient during immersion frying. *Journal of Food Process Engineering,* 22: 201-214.

Hwang, M.P. and K. Hayakawa. 1979. A specific heat calorimeter for foods. *Journal of Food Science*. 44(2): 435-438.

Kazarian, E.A. and C.W. Hall. 1965. Thermal properties of grains. *Transactions of ASAE*, 8(1): 33-48.

Kestin, J and W.A. Wakeham. 1988. *Transport Properties of Fluids: Thermal Conductivity, Viscosity and Diffusion Coefficient Vol. I-1.* Cindas data series on material properties. ed. C.Y Ho, 221. New York, NY: Hemisphere Publishing Corporation.

Kramkowski, R., E. Kamiński and M. Serowik. 2001. Effect of moisture and temperature of garlic on its specific heat*. Electronic Journal of Polish Agricultural Universities: Agricultural Engineering Series*, 4(2).

Krokida, M.K., V. Oreopoulou and Z.B. Maroulis. 2000. Water loss and oil uptake as a function of frying time. *Journal of Food Engineering*. 44: 39-46.

Matthews, F.V. Jr. and C.W. Hall. 1968. Method of finite differences used to relate changes in thermal and physical properties of potatoes. *Transaction of ASAE*, 11: 558.

Miller, K.S., R.P. Singh and B.E. Farkas. 1994. Viscosity and heat transfer coefficients for canola, corn, palm and soybean oil. *Journal of Food Processing and Preservation,* 18: 461-472.

Mittelman, N., S. Mizrahi and Z. Berk. 1984. Heat and mass transfer in frying. In *Engineering and Food, Engineering Sciences in the Food Industry*. Volume I. ed. McKenna B., 109–116. London, UK: Elsevier Science ad Technology Books.

Mohsenin, N.N. 1970. *Physical Properties of Plant and Animal Materials* New York, NY: Gordon and Breach Science Publishers.

Moriera. R. G., Barrufet, M.A. and M.E. Castell-Perez. 1999. *Deep Fat Frying: Fundamentals and Applications.* New York, NY: Kluwer Academic Publishers.

Moreira, R.G., J. Palau, V.E. Sweat and X. Sun. (1995a). Thermal and physical properties of tortilla chips as a function of frying time. *Journal of Food Processing and Preservation*, 19: 175-189.

Moreira, R. G., J.E Palau and X Sun. 1995b. Deep fat frying of tortilla chips: an engineering approach. *Food Technology,* 49: 146-150.

Murakami, E.G. and M.R. Okos. 1989. Measurement and predictions of thermal properties of foods. In *Food Properties and Computer Aided Engineering of Food Processing Systems*. ed. R.P. Singh and A. G. Medina. New York, NY: Kluwer Academic Publishers.

Ni, H. and A.K. Datta. 1999. Moisture, oil and energy transport during deep-fat frying of food materials. *Transactions of Institution of Chemical Engineers. Part C: Food and Bioproducts Processing,* 77: 194–204.

Picha, D. H. 1985. Crude protein, minerals and total carbtenoids in sweet potatoes. *Journal of Food Science*, 50: 1768.

Rahman, S. 1995. *Food properties handbook.* 192. New York, NY: CRC Press.

Rice, P. and M.H. Gamble. 1989. Technical note: modeling moisture loss during potato slice frying. *Journal of Food Science and Technology,* 24: 183–187.

Rice, P., J.D. Selman and R.K. Abdul-Rezzak. 1988. Effect of temperature on thermal properties of ‘Record’ potatoes. *International Journal of Food Science and Technology.* 23:281-286.

Rodriguez, R., B.L. Raina, E.B. Pantatisco and M.B. Bhatti. 1975. *Quality of Raw Material for Processing in Post harvest Physiology: Handling and Utilization of Tropical and Subtropical Fruits and Vegetable.* ed. E.B. Pantatisco, 467. Westport CT: AVI Publishing Co.

Sabapathy N. D. 2005. Heat and mass transfer during cooking of chickpea-measurements and computational simulation. Unpublished M.Sc Thesis. Saskatoon, SK: University of Saskatchewan.

Saravacos, G.D. and M.N. Pilsworth. 1965. Thermal conductivity of freeze-dried model food gels. *Journal of Food Science*, 30: 773-778.

Scheerlinck, N., B.M. Nicolai, P. Verboven and J. De Baerdemaeker. 1996. Finite element analysis of coupled heat and mass transfer problems with

random field material properties. ASAE Paper No. 96-3028. St. Joseph, MI: American Society of Agricultural Engineers.

Siebel, E. 1892. Specific heat of various products. *Ice and Refrigeration*. 2: 256-257.

Stitt, F. and E. K. Kennedy. 1945. Specific heats of dehydrated vegetables and egg powder. *Food Research*, 10: 426- 436.

Stroshine, R. 1998. *Physical Properties of Agricultural Materials and Food Products*. West Lafayette, IN: Purdue University.

Sweat, V.E. 1986. Thermal properties of foods, In *Engineering Properties of Foods.* ed. M.A Rao, and S.S.H. Rizvi, 49-87. New York, NY: Marcel and Dekker Inc.

Tang, J., S. Sokhansanj, S. Yannacopoulos and S. O. Kasap. 1991. Specific heat capacity of lentil seeds by differential scanning calorimetry. *Transactions of ASAE*. 34(2): 517-522.

Tong, L.S., Y.S. Tang. 1997. *Boiling Heat Transfer and Two-Phase Flow*, 2nd edition. Washington D.C.: Taylor and Francis.

USDA. 1963. Agriculture Handbook No. 8: Composition of Foods; Raw, Processed, Prepared. Washington, DC. United States Department of Agriculture.

USDA. 1984. Potatoes and Sweetpotatoes: Final Estimate. Statistical Bulletin 1978-1982. 709. Washington, DC.

Wadsworth, J.I. and J.J. Spadaro. 1969. Transient temperature distribution in whole sweet potato roots during immersion heating. *Food Technology,* 23: 219.

Wang, N. and J.G. Brennan. 1992. Thermal conductivity of potato as a function of moisture content. *Journal of Food Engineering*, 17: 153-160.

Wang, N. and J.G. Brennan. 1993. The influence of moisture content and temperature on the specific heat of potato measured by differential scanning calorimetry. *Journal of Food Engineering*, 19: 303-310.

Woodside, W. and J.H. Messmer. 1961. Thermal conductivity of porous media. I. Unconsolidated sands. *Journal of Applied Physics.* 1688.

APPENDICES

APPENDIX A

Table A1. Density of sweetpotato determined by Multipycnometer.

Moisture content (w.b)	Trials I	II	III	IV	V
	Density (kg/m^3)				
0.75	1126	1122	1125	1118	1124
0.65	1189	1171	1182	1194	1201
0.55	1241	1218	1263	1233	1255
0.45	1298	1312	1284	1301	1277

C.V = 1.03, RMSE = 12.49

Table A2. Specific heat of sweetpotato determined by DSC.

M.C	0.75		0.65		0.55		0.45	
Trials	I	II	I	II	I	II	I	II
Temp. (°C)								
20	3088.1	2912.4	2864.5	2881.6	2458.2	2424.6	2297.8	2285
30	3123.5	2933.4	2889.7	2901.4	2486.7	2434.5	2314.6	2294.6
40	3164	2968.4	2902.4	2924.5	2503.1	2454.6	2339.2	2308.4
50	3259.7	3119.9	2957.2	2979.8	2581.1	2485.5	2340.2	2351.8
60	3292.1	3158.4	3003.5	2944.2	2623.9	2557.4	2364.1	2403.1
70	3303.4	3124.2	3020.5	2925.3	2638.4	2599.5	2409.3	2450.8
80	3313.8	3165.0	3035.8	2970.8	2644.3	2631.3	2454.4	2472
90	3323	3165.9	3056.6	2975.6	2657.2	2660.4	2503	2482.3
100	3329.7	3190	3100.4	2993.5	2804	2816.3	2626.4	2630.7
110	3350	3261.8	3167.8	3090.6	2870.6	2910.5	2754.1	2791.5
120	3385.2	3283.7	3220.8	3143.2	2940.5	2963.2	2881.3	2840.7
130	3392.5	3301.4	3221.8	3170.8	2933.5	2973.4	2891	2867.8
140	3399.5	3378.4	3240	3216.4	2970.6	2975.4	2900.1	2888
150	3429.1	3416	3301.8	3275.4	3016.1	3024.8	2954.6	2966.6
160	3477	3481.2	3342.5	3333.5	3051.6	3081.4	3002	2998.4
170	3523.8	3498.3	3377.3	3381.5	3122.4	3111.6	3044.5	3065.1
180	3566.2	3539.4	3401.5	3397	3201.1	3176.9	3089.4	3077.6

C.V = 4.33, RMSE = 123

Table A3. Moisture content of sweetpotato during frying (decimal, wet basis) – Trial1

Temp. (°C)	150			160			170			180		
Sizes	I	II	III	I	II	III	I	II	III	I	II	III
Whole												
Time (s)												
30	0.791	0.780	0.781	0.786	0.782	0.784	0.790	0.778	0.780	0.749	0.764	0.777
60	0.760	0.748	0.748	0.758	0.746	0.746	0.760	0.741	0.744	0.705	0.722	0.732
120	0.729	0.721	0.721	0.726	0.717	0.717	0.709	0.704	0.702	0.658	0.683	0.691
180	0.697	0.689	0.687	0.694	0.679	0.678	0.681	0.661	0.667	0.611	0.646	0.654
240	0.675	0.664	0.657	0.670	0.648	0.647	0.658	0.641	0.641	0.587	0.620	0.631
300	0.667	0.647	0.649	0.656	0.637	0.641	0.634	0.633	0.633	0.583	0.614	0.626
Crust												
Time (s)												
30	0.676	0.748	0.760	0.689	0.721	0.701	0.693	0.698	0.702	0.631	0.666	0.682
60	0.601	0.668	0.689	0.595	0.654	0.680	0.532	0.614	0.616	0.425	0.505	0.531
120	0.537	0.577	0.586	0.474	0.517	0.557	0.382	0.468	0.473	0.278	0.381	0.394
180	0.423	0.466	0.455	0.358	0.412	0.406	0.271	0.335	0.332	0.234	0.279	0.308
240	0.338	0.387	0.376	0.297	0.333	0.358	0.244	0.279	0.314	0.228	0.253	0.283
300	0.327	0.343	0.363	0.266	0.272	0.312	0.233	0.256	0.304	0.208	0.234	0.243
Core												
Time (s)												
30	0.818	0.815	0.813	0.819	0.806	0.813	0.803	0.803	0.813	0.802	0.801	0.815
60	0.803	0.811	0.810	0.818	0.799	0.805	0.799	0.799	0.804	0.798	0.799	0.799
120	0.799	0.795	0.805	0.802	0.798	0.799	0.798	0.796	0.793	0.786	0.791	0.794
180	0.798	0.789	0.798	0.795	0.787	0.796	0.782	0.788	0.788	0.779	0.786	0.780
240	0.781	0.787	0.783	0.771	0.783	0.791	0.776	0.783	0.782	0.769	0.776	0.777
300	0.779	0.780	0.781	0.769	0.779	0.787	0.772	0.779	0.773	0.762	0.762	0.762

Sizes: I is (D/L=2.5), II is (D/L=3.5), III is (D/L=4)

Table A4. Moisture content of sweetpotato during frying (decimal, wet basis) – Trial 2

Temp. (°C)	150			160			170			180		
Sizes	I	II	III	I	II	III	I	II	III	I	II	III
Whole												
Time (s)												
30	0.783	0.775	0.794	0.781	0.779	0.791	0.786	0.782	0.789	0.754	0.768	0.781
60	0.744	0.735	0.759	0.751	0.737	0.754	0.760	0.752	0.751	0.709	0.721	0.738
120	0.708	0.700	0.723	0.723	0.706	0.716	0.716	0.709	0.713	0.661	0.687	0.693
180	0.682	0.671	0.696	0.698	0.678	0.682	0.684	0.662	0.677	0.616	0.647	0.663
240	0.662	0.648	0.670	0.670	0.651	0.652	0.657	0.636	0.648	0.591	0.621	0.636
300	0.651	0.643	0.643	0.645	0.641	0.646	0.633	0.631	0.642	0.589	0.615	0.629
Crust												
Time (s)												
30	0.731	0.750	0.764	0.693	0.724	0.724	0.697	0.702	0.706	0.636	0.670	0.686
60	0.626	0.652	0.694	0.568	0.641	0.683	0.536	0.619	0.621	0.489	0.509	0.553
120	0.521	0.579	0.612	0.478	0.535	0.559	0.386	0.470	0.478	0.324	0.381	0.425
180	0.422	0.470	0.459	0.361	0.417	0.410	0.327	0.368	0.350	0.239	0.282	0.312
240	0.341	0.391	0.380	0.285	0.335	0.362	0.276	0.282	0.312	0.233	0.255	0.297
300	0.320	0.347	0.367	0.269	0.35	0.337	0.237	0.261	0.286	0.225	0.238	0.247
Core												
Time (s)												
30	0.807	0.810	0.813	0.804	0.806	0.811	0.801	0.808	0.812	0.800	0.799	0.804
60	0.803	0.809	0.809	0.802	0.805	0.805	0.796	0.799	0.803	0.796	0.794	0.798
120	0.801	0.7800	0.803	0.792	0.798	0.799	0.787	0.796	0.794	0.784	0.790	0.795
180	0.796	0.793	0.797	0.782	0.789	0.793	0.780	0.787	0.790	0.777	0.777	0.785
240	0.785	0.786	0.788	0.774	0.786	0.791	0.772	0.784	0.781	0.770	0.766	0.771
300	0.784	0.779	0.785	0.773	0.778	0.781	0.771	0.773	0.773	0.766	0.762	0.766

Sizes: I is (D/L=2.5), II is (D/L=3.5), III is (D/L=4)

Table A5. Temperature of sweetpotato sample during frying - Trial 1

Temp. (°C)	150			160			170			180		
Sizes	I	II	III	I	II	III	I	II	III	I	II	III
Top												
Time (s)												
0	23.05	22.53	23.71	21.58	22.73	23.01	22.91	23.04	21.60	22.60	22.81	22.78
30	125.3	126.4	119.0	135.2	149.5	145.3	151.2	150.5	157.3	161.3	158.5	158.6
60	134.2	136.3	130.2	143.9	152.1	149.5	160.5	157.0	159.8	165.6	165.3	163.3
120	139.8	140.1	134.2	149.5	152.2	152.6	160.4	160.0	163.0	167.4	166.2	168.3
180	142.6	143.0	135.6	149.9	151.9	151.1	161.4	161.3	162.3	169.3	168.0	167.8
240	143.8	141.9	135.7	147.5	152.8	150.2	161.5	161.5	162.2	170.6	170.0	167.9
300	143.7	142.7	136.2	148.3	153.2	150.2	163.0	161.9	163.6	169.5	170.6	170.2
T2 (Between Top and Center)												
Time (s)												
0	22.60	23.11	24.04	22.19	22.03	22.21	22.35	22.82	21.03	22.60	23.22	23.02
30	63.15	70.03	74.70	71.13	71.52	78.05	69.60	75.12	76.25	71.60	92.00	85.00
60	90.60	90.45	92.30	93.75	89.00	95.35	94.75	91.52	93.30	94.90	100.1	98.25
120	102.4	99.55	101.5	103.4	100.8	101.0	103.0	105.1	101.8	104.8.	107.4	105.2
180	113.4	108.6	104.8	112.1	114.6	106.4	112.6	113.6	116.8	115.3	119.1	120.1
240	122.6	122.7	112.1	125.8	125.9	115.8	126.0	124.4	130.6	127.6	132.2	135.6
300	128.3	128.2	121.9	133.5	132.8	124.9	136.5	131.4	136.5	135.8	139.8	145.6
Center												
Time (s)												
0	22.46	22.51	24.05	20.58	23.19	22.99	22.05	23.58	21.11	22.35	22.90	22.71
30	50.51	48.75	54.05	40.15	42.79	47.11	53.83	63.12	36.07	49.69	62.34	53.30
60	82.60	72.45	78.75	71.07	69.46	73.35	80.75	85.75	67.80	81.25	85.00	80.50
120	99.51	98.50	99.25	98.91	98.30	99.61	101.7	100.5	98.40	103.1	101.0	102.6
180	101.1	101.3	100.9	101.9	101.4	100.9	103.8	102.7	101.7	103.2	102.5	104.8
240	102.0	103.3	101.2	101.6	101.6	101.5	104.9	103.9	102.9	104.9	104.7	108.1
300	102.8	105.0	101.6	101.6	102.6	103.2	106.4	105.2	106.0	107.3	108.8	113.0
T4 (Between Center and Bottom)												
Time (s)												
0	22.50	22.55	23.52	21.22	23.29	23.06	22.61	23.15	20.85	22.89	23.09	23.09
30	76.35	73.05	74.20	67.37	83.05	77.80	74.00	77.20	72.77	83.00	85.25	81.20
60	93.00	88.80	99.80	88.65	94.30	91.85	92.15	90.65	89.15	97.20	96.50	95.05
120	101.8	100.4	99.61	100.5	103.0	102.7	102.5	102.0	100.2	105.4	105.9	103.6
180	113.5	111.6	105.2	113.1	114.7	110.9	116.2	110.1	117.1	116.9	114.6	118.9
240	123.3	123.1	115.7	125.8	125.0	117.4	130.1	122.0	130.1	129.5	128.9	131.8
300	128.0	129.5	123.6	134.8	130.6	124.5	138.5	128.7	133.5	139.6	136.8	140.7
Bottom												
Time (s)												
0	23.24	23.05	23.74	21.55	23.03	23.03	23.08	23.20	22.01	23.62	23.05	23.01
30	130.3	132.8	132.1	127.3	150.3	154.0	143.0	156.7	154.3	151.0	162.2	153.7
60	134.0	136.0	134.7	135.5	153.4	154.2	152.2	161.8	161.7	160.2	168.3	160.2
120	138.9	140.5	135.5	147.0	154.1	153.6	157.0	161.6	163.7	162.6	167.5	169.5
180	142.8	143.6	139.2	150.8	154.2	153.6	158.7	163.0	164.9	166.1	171.4	170.2
240	143.5	143.3	139.4	150.7	153.2	15.44	160.7	162.9	164.0	168.6	173.1	169.4
300	143.5	143.8	138.4	150.2	154.4	154.6	161.6	164.4	164.5	169.0	172.9	173.5

Table A6. Temperature of sweetpotato sample during frying - Trial 2

Temp. (°C)	150			160			170			180		
Sizes	I	II	III	I	II	III	I	II	III	I	II	III
Top												
Time (s)												
0	24.45	23.93	25.01	22.98	23.60	23.21	23.91	23.04	22.58	23.75	23.05	23.07
30	126.5	127.8	120.5	136.2	149.1	145.7	151.2	151.2	158.3	161.4	158.9	158.5
60	135.3	137.3	131.2	144.8	151.6	150.6	161.1	156.9	159.8	165.5	165.4	163.2
120	139.6	140.0	134.1	149.4	151.4	153.4	161.5	160.8	162.5	167.6	165.9	167.4
180	141.6	142.0	134.6	149.2	151.1	151.2	161.9	160.9	161.9	169.5	167.8	168.2
240	142.6	141.7	134.8	147.2	152.8	150.8	162.1	160.9	162.7	170.1	169.6	168.3
300	141.9	141.3	135.1	147.8	152.1	150.7	162.3	161.8	162.9	169.9	169.8	169.5
T2 (Between Top and Center)												
Time (s)												
0	22.81	23.70	24.04	22.69	21.73	23.02	23.85	23.02	21.13	23.70	23.22	23.92
30	63.05	70.68	75.10	71.73	70.98	78.25	70.60	77.72	76.25	71.60	92.90	84.80
60	90.81	89.95	91.19	96.25	90.66	96.35	93.64	93.62	93.30	94.57	101.6	99.75
120	103.8	98.66	101.4	104.9	101.9	103.4	101.4	103.5	101.9	104.4	109.0	106.2
180	111.8	107.9	102.4	112.2	115.6	106.3	114.9	112.8	114.9	113.9	119.6	120.2
240	123.9	124.2	113.3	127.8	123.5	114.4	126.8	124.6	131.8	128.6	130.6	137.5
300	127.2	127.5	121.9	133.9	131.8	125.9	135.2	130.9	134.6	135.4	138.4	143.8
Center												
Time (s)												
0	23.86	24.21	23.75	22.28	23.59	23.79	22.85	24.58	21.71	22.95	22.56	23.62
30	51.70	49.65	54.55	41.75	43.49	47.91	55.33	64.12	35.99	50.49	62.96	53.80
60	83.40	73.05	79.25	72.37	69.86	74.15	81.35	87.25	69.33	81.85	85.66	81.60
120	98.91	99.10	99.75	99.40	98.88	101.1	103.1	101.1	99.32	104.5	101.7	102.9
180	101.3	101.1	101.4	102.1	100.9	101.4	103.5	102.5	101.8	104.7	103.3	104.6
240	101.7	103.2	101.6	102.0	101.5	102.0	104.6	103.2	102.3	105.3	105.1	107.8
300	102.3	104.7	101.9	101.9	102.1	102.5	105.9	104.8	105.6	106.6	107.1	113.4
T4 (Between Center and Bottom)												
Time (s)												
0	22.85	23.65	24.52	22.21	22.99	23.12	23.81	23.45	21.70	23.79	23.89	23.81
30	76.75	73.65	74.70	67.54	83.65	78.63	74.40	77.60	74.17	83.20	85.95	81.80
60	94.50	89.30	90.60	89.55	95.20	92.77	92.11	91.45	90.55	97.90	97.04	94.94
120	101.8	101.3	101.5	101.2	104.1	103.5	103.3	102.3	101.6	104.0	106.6	104.3
180	113.6	111.4	105.6	112.4	114.8	111.2	116.5	110.9	116.1	117.4	114.0	118.4
240	123.1	122.5	115.2	125.2	125.5	117.1	130.4	121.1	130.1	128.9	128.3	131.5
300	127.5	129.3	122.9	133.3	129.8	124.0	138.7	128.6	132.9	139.1	135.9	141.1
Bottom												
Time (s)												
0	23.74	23.75	24.64	22.05	22.83	23.53	23.28	23.60	22.71	24.82	23.25	23.81
30	131.2	131.4	133.3	127.6	151.2	154.4	143.5	157.4	155.1	150.5	163.0	154.3
60	134.8	136.5	135.7	136.3	154.3	154.4	153.1	162.5	162.7	160.4	168.5	161.2
120	140.2	140.5	135.9	147.8	154.7	154.5	157.1	162.2	164.4	162.9	168.2	170.0
180	142.8	143.9	138.4	149.6	153.8	153.8	158.2	162.6	164.6	165.7	171.1	169.9
240	142.9	144.2	139.6	149.9	153.6	154.9	159.9	162.6	163.9	168.2	172.4	171.1
300	143.3	143.5	140.7	150.1	153.9	154.4	161.0	163.4	163.9	168.6	172.6	172.8

Table A7. Average heat transfer coefficient during frying (W/m^2°C) - Trial 1

Temp. (°C)	150			160			170			180		
Sizes	I	II	III	I	II	III	I	II	III	I	II	III
Time (s)												
30	136.8	103.0	103.0	146.9	109.5	109.3	144.8	109.8	108.5	125.3	125.8	125.3
60	597.3	599.8	583.5	644.0	596.3	597.9	726.0	725.1	746.0	796.1	796.2	800.3
120	696.1	680.5	714.0	722.9	713.1	726.0	680.0	690.6	767.0	646.8	738.3	755.5
180	551.2	531.6	585.9	546.7	488.4	493.0	624.2	507.7	618.5	503.7	525.2	559.1
240	474.3	481.9	562.2	518.5	483.1	502.1	572.8	504.6	527.3	491.2	513.2	509.3
300	441.1	467.5	538.9	502.1	439.0	486.0	498.7	461.2	511.2	429.0	463.7	477.9

Sizes: I is (D/L=2.5), II is (D/L=3.5), III is (D/L=4)

Table A8. Average heat transfer coefficient during frying (W/m^2°C) - Trial 2

Temp. (°C)	150			160			170			180		
Sizes	I	II	III	I	II	III	I	II	III	I	II	III
Time (s)												
30	131.2	100.3	102.3	139.5	107.7	108.3	142.2	109.4	106.4	124.5	120.9	124.3
60	615.8	585.9	489.7	688.6	593.5	589.5	760.7	749.9	750.1	837.5	805.7	804.5
120	710.7	700.6	674.5	715.2	697.1	720.2	666.2	692.2	627.4	674.8	764.2	781.7
180	512.9	503.5	527.5	476.5	545.8	551.7	574.6	531.4	550.5	503.6	577.7	599.0
240	508.0	496.3	539.6	554.1	459.5	447.1	561.2	529.8	533.8	478.9	574.7	512.0
300	400.3	451.8	512.5	505.5	473.7	436.8	514.9	507.7	443.9	430.7	523.9	485.5

Sizes: I is (D/L=2.5), II is (D/L=3.5), III is (D/L=4)

Table A9. Average mass transfer coefficient during frying ($kg/m^2.s$) – Trial 1

Size	I	II	III
Temp. (°C)			
150			
Time (s)			
0-30	2.70×10^{-6}	1.40×10^{-6}	9.00×10^{-6}
30-60	3.00×10^{-6}	2.00×10^{-6}	1.80×10^{-6}
60-120	3.00×10^{-6}	2.20×10^{-6}	2.20×10^{-6}
120-180	4.40×10^{-6}	4.05×10^{-6}	4.60×10^{-6}
180-240	4.90×10^{-6}	4.00×10^{-6}	4.50×10^{-6}
240-360	4.00×10^{-6}	4.00×10^{-6}	3.20×10^{-6}
160			
Time (s)			
0-30	2.70×10^{-6}	1.00×10^{-6}	2.00×10^{-6}
30-60	3.20×10^{-6}	3.00×10^{-6}	2.00×10^{-6}
60-120	4.50×10^{-6}	3.00×10^{-6}	2.60×10^{-6}
120-180	5.70×10^{-6}	4.80×10^{-6}	5.20×10^{-6}
180-240	5.40×10^{-6}	4.70×10^{-6}	3.90×10^{-6}
240-360	5.40×10^{-6}	4.20×10^{-6}	3.50×10^{-6}
170			
Time (s)			
0-30	2.70×10^{-6}	2.50×10^{-6}	2.10×10^{-6}
30-60	6.20×10^{-6}	2.20×10^{-6}	2.40×10^{-6}
60-120	6.70×10^{-6}	5.60×10^{-6}	4.50×10^{-6}
120-180	7.00×10^{-6}	5.90×10^{-6}	6.10×10^{-6}
180-240	6.50×10^{-6}	5.90×10^{-6}	4.20×10^{-6}
240-300	6.00×10^{-6}	5.70×10^{-6}	4.20×10^{-6}
180			
Time (s)			
0-30	4.50×10^{-6}	3.90×10^{-6}	2.60×10^{-6}
30-60	6.40×10^{-6}	5.10×10^{-6}	4.10×10^{-6}
60-120	6.90×10^{-6}	5.50×10^{-6}	5.70×10^{-6}
120-180	7.30×10^{-6}	6.30×10^{-6}	6.60×10^{-6}
180-240	6.70×10^{-6}	7.20×10^{-6}	5.50×10^{-6}
240-300	5.40×10^{-6}	5.90×10^{-6}	5.50×10^{-6}

Sizes: I is (D/L=2.5), II is (D/L=3.5), III is (D/L=4)

Table A10. Average mass transfer coefficient during frying ($kg/m^2.s$) – Trial 2

Size	I	II	III
Temp. (°C)			
150			
Time (s)			
0-30	2.00×10^{-6}	1.40×10^{-6}	9.00×10^{-6}
30-60	2.40×10^{-6}	2.10×10^{-6}	1.60×10^{-6}
60-120	3.30×10^{-6}	2.20×10^{-6}	1.80×10^{-6}
120-180	4.60×10^{-6}	4.00×10^{-6}	4.40×10^{-6}
180-240	5.30×10^{-6}	4.00×10^{-6}	4.40×10^{-6}
240-360	4.00×10^{-6}	4.00×10^{-6}	3.00×10^{-6}
160			
Time (s)			
0-30	2.60×10^{-6}	1.40×10^{-6}	1.40×10^{-6}
30-60	4.10×10^{-6}	3.00×10^{-6}	1.50×10^{-6}
60-120	4.30×10^{-6}	3.00×10^{-6}	2.90×10^{-6}
120-180	5.80×10^{-6}	4.70×10^{-6}	5.20×10^{-6}
180-240	5.60×10^{-6}	4.70×10^{-6}	3.90×10^{-6}
240-360	5.50×10^{-6}	4.20×10^{-6}	3.50×10^{-6}
170			
Time (s)			
0-30	2.70×10^{-6}	2.30×10^{-6}	1.80×10^{-6}
30-60	6.20×10^{-6}	2.40×10^{-6}	2.60×10^{-6}
60-120	6.50×10^{-6}	5.00×10^{-6}	4.50×10^{-6}
120-180	6.90×10^{-6}	5.40×10^{-6}	6.10×10^{-6}
180-240	6.40×10^{-6}	5.70×10^{-6}	5.00×10^{-6}
240-300	6.00×10^{-6}	5.20×10^{-6}	4.70×10^{-6}
180			
Time (s)			
0-30	4.50×10^{-6}	3.90×10^{-6}	2.60×10^{-6}
30-60	6.30×10^{-6}	5.20×10^{-6}	4.40×10^{-6}
60-120	6.70×10^{-6}	6.20×10^{-6}	5.50×10^{-6}
120-180	7.20×10^{-6}	7.10×10^{-6}	6.60×10^{-6}
180-240	6.70×10^{-6}	6.10×10^{-6}	5.40×10^{-6}
240-300	5.40×10^{-6}	5.80×10^{-6}	5.40×10^{-6}

Sizes: I is (D/L=2.5), II is (D/L=3.5), III is (D/L=4)

Table B1. Summarised ANOVA table for empirical correlation between heat transfer coefficient, h and mass transfer coefficient, h_m at maximum h.

Source	DF	Sum of Squares	Mean Square	F Value	Pr > F
h	1	37.7	37.7	720.3	<.0001
h*h	1	5.4	5.4	102.6	<.0001

D.F. of error = 21

Table B2. Summarised ANOVA table for empirical correlation between maximum heat transfer coefficient, h and maximum coefficient, h_m.

Source	DF	Sum of Squares	Mean Square	F Value	Pr > F
h	1	45.5	45.5	599.2	<.0001
h*h	1	8.7	8.7	88.3	<.0001

D.F. of error = 21

Table B3. Summarised ANOVA table for effect of oil temperature, sample size and frying progression on heat transfer coefficient during frying.

Source	DF	Sum of Squares	Mean Square	F Value	Pr > F
T_{oil}	1	55958.4	55958.4	17.9	<.0001
$\Delta T^* T_{oil}$	1	695955.8	695955.8	222.1	<.0001
ΔT^2	1	1485064.4	1485064.4	473.9	<.0001
$d^* T_{oil}$	1	15219.8	15219.8	11.3	0.0085

D.F. of error = 115

Table B4. Summarised ANOVA table for effect of oil temperature, sample size and frying progression on mass transfer coefficient during frying.

Source	DF	Sum of Squares	Mean Square	F Value	Pr > F
T_{oil}	1	1.77×10^{-10}	1.77×10^{-10}	210.81	<.0001
d	1	6.34×10^{-11}	6.34×10^{-11}	75.27	<.0001
ΔT	1	1.57×10^{-10}	1.57×10^{-10}	86.10	<.0001
ΔT^2	1	4.98×10^{-12}	4.98×10^{-12}	5.92	0.0163

D.F. of error = 115